DEVELOPMENT OF CLOSED SPACE SUBLIMATION TECHNIQUE AND PREPARATION OF Cd-BASED THIN FILMS

By

Sajid Butt

School of Chemical and Materials Engineering

National University of Sciences and Technology (NUST),

Islamabad, Pakistan

2010

DEVELOPMENT OF CLOSED SPACE SUBLIMATION TECHNIQUE AND PREPARATION OF Cd-BASED THIN FILMS

Defining futures

By

SAJID BUTT

(**MS Session: 2008-2010**)

Supervised By

Prof. Dr. ASGHARI MAQSOOD

Co-Supervisor

Dr. N.A. Shah

This work is submitted as a dissertation in partial fulfillment of the requirement for the degree of

MASTERS OF SCIENCE (MS)

In

MATERIALS AND SURFACE ENGINNERING

School of Chemical and Materials Engineering

National University of Sciences and Technology (NUST), H-12, Islamabad, Pakistan

Certificate

This is to certify that the work in this dissertation has been carried out by Sajid Butt and completed under my supervision at Thermal Transport Laboratory, School of Chemical and Materials Engineering, National University of Sciences and Technology, Islamabad, Pakistan

Prof. Dr. Asghari Maqsood
Supervisor
Thermal Transport Laboratory,
School of Chemical and Materials Engineering,
National University of Sciences and Technology,

Dr. N.A.Shah
Co-Supervisor
Department of Physics
COMSATS Institute of Information Technology, Islamabad, Pakistan

Submitted through

Prof. Dr. M. Mujahid
HoD: Materials Department
School of Chemical and Materials Engineering,
National University of Sciences and Technology,
Islamabad, Pakistan

بِسْمِ اللهِ الرَّحْمٰنِ الرَّحِيْمِ

In the name of ALLAH, the Beneficent, the Merciful.

عَلَّمَ الْإِنسَانَ مَا لَمْ يَعْلَمْ ۝٥

"He teacheth man that which he knew not"

ACKNOWLEDGEMENTS

It gives me a great pleasure and satisfaction to acknowledge the endowment of the creator of the universe, Allah Almighty, the most gracious, compassionate and beneficent to His creature, Who favoured man by sending His last Prophet, Muhammad (P.B.U.H) who is forever a source of guidance and knowledge for humanity.

I wish to thank my supervisor Prof. Dr. Asghari Maqsood for all of her support, advice and guidance. I especially wish to thank her for the generosity she showed with her time and she was always willing to talk. I would also like to thank my co-supervisor, Dr. Nazar Abbas Shah who guided and facilitated me a lot while doing experimental work in his laboratory.

I am grateful to Engr. Salman Absar DG SCME for giving permission to work with full liberty even after working hours. I am very thankful to Prof. Dr. M. Bilal Khan Dean SCME, who always patted me on the shoulder and gave moral support. He always encourages students to work for the betterment of human being. I am thankful to Prof. Dr. M. Mujahid HOD Materials Department, for providing access to departmental facilities and his useful guidance to interpret SEM & EDX results. I am extremely thankful to Dr. Zulfiqar for guiding me about optical characterizations and Mr. Mohammad Ashraf for giving technical support, Optics Laboratory, Islamabad. I will always remember the assistance of Mr. Shams-Ud-Din, SEM Laboratory, and Mr. Khalid Akbar, XRD Laboratory SCME while working in their laboratories. I regards to all of my teachers, especially Dr. Mohammad Islam for fruitful discussion with him. I acknowledge the help of Dr. M. Anis-Ur-Rehman regarding XRD, Thermal Physics Laboratory, COMSATS and Ms Naghma, XRD Laboratory, Minerals Laboratory for her guidance.

I will never forget the cooperation of my Laboratory fellows especially Mr. Adnan and Mr. Rizwan and other laboratory attendants. I am thankful to all of my class fellows specially Mr. Aftab Akram for very useful discussion with him. I am thankful to my room-mates, Muhammad Umer Farooq and Rana Usman Ali for their company and patience during research days. I am also thankful to my colleague Bilal Ahmad Khan, IST, for his nice company and guidance.

I have no words to describe my sensation of respect about my family, who remembered me in their prayers, without their shadow of love; perhaps it could not be possible for me to attain this target. May Allah bless them with health, wealth, happiness and faith!

My special thanks to NUST, Pakistan Atomic Energy Commission and Higher Education Commission for providing their generous technical and financial support.

Sajid Butt

DEDICATED TO

My parents (late), May Allah bless them

and

My loving family who always supported me and prayed for me

DEVELOPMENT OF CLOSED SPACE SUBLIMATION TECHNIQUE AND PREPARATION OF Cd-BASED THIN FILMS

Sajid Butt, Thermal Transport Laboratory, SCME, NUST, Islamabad, Pakistan

ABSTRACT

In the present work, a coating unit for depositing thin films has been developed which works on the technique "Closed Space Sublimation" in which a powdered material is deposited under vacuum. Cadmium Sulfide thin films has been deposited on a glass substrate. Structural, morphological, compositional, optical, and electrical properties of the samples have been determined before and after Indium doping. The main goal doping is to get comparatively high electrically conductive films. The optical properties of the films are also very important from the application point of view so that improvement in conductivity should not be associated at the expense of optical and structural properties of the films.

The structure of the films was studied by XRD, SEM and composition of the films was measured by EDX. A model was used for the calculation of optical parameters (optical band gap, refractive index, and films thickness) from the optical transmission spectra recorded by spectrophotometer. Samples of different thickness ranging from 250nm to 900nm were obtained and most of the samples have a band gap near 2.4eV before and after doping, calculated from the transmission data obtained from spectrophotometer.

To reduce the resistivity of the thin films, Indium was doped. Indium was thermally evaporated and annealed at different temperatures in order to diffuse it in as-deposited CdS samples. XRD results confirmed the diffusion and formation of new compounds of indium with cadmium sulfide. Resistivity of 10^{-1} to 10^{-2} Ωcm was obtained.

TABLE OF CONTENTS

LIST OF FIGURES

LIST OF TABLES

CHAPTER 1

VACUUM SCIENCE AND TECHNOLOGY

Virtually all thin-film deposition and processing methods as well as techniques employed to characterize and measure the properties of films require a vacuum or some sort of reduced pressure environment. For this reason the relevant aspects of vacuum science and technology are being discussed in this chapter [1]. Moreover, Closed Space Sublimation (CSS) unit for fabrication of thin films has been built and installed under this research work, which is also a type of vacuum evaporation, will be discussed in details in chapters 5.

1.1. THE VACUUM

A vacuum is a space from which air or other gases have been removed, or the pressure of the gas in the enclosure has been reduced to less than the atmospheric pressure. In technical terms, the vacuum refers to a given space filled with a gas having a density of molecules less than 2.5×10^{19} molecules/ cm^3 at normal temperature.

1.2. THE NEED OF VACUUM

Nowadays, vacuum is utilized in the following situations:

- To avoid collisions
- To remove dissolved gases
- To reduce the energy transfer
- To achieve Pressure difference
- To produce contamination free surfaces
- To remove active atmospheric constituents
- To reduce the boiling points (helps in sublimation as well)

1.3. VARIOUS UNITS OF VACUUM

The pressure of a gas, defined in terms of gas impingement on a surface is the time rate of change of the normal component of momentum of the impinging gas molecules per unit area of surface (force per unit area) [1].

Table 1.1:
Various units for pressure measurement

System	Unit of area	Unit of force	Unit of pressure
CGS	cm^2	Dyne 1dyne = 1 g cm/s^2	$dyne/cm^2$ 1 bar = 10^6 $dyne/cm^2$ = 10^5 N/m^2
SI (MKS)	m^2	Newton (N) 1 N = 1 kg m/s^2	N/m^2 1Pascal (Pa) = 1 N/m^2
Technical	cm^2	Kgf 1 kgf = 9.81 N	Kgf/cm^2 1 atm = $1kgf/cm^2$ = 9.81×10^4 N/m^2
British	ft^2 in^2	1 lbf ≈ 4.448 N	$lbf/ft^2 \approx 47.88$ N/m^2 psi = $lbf/in^2 \approx 6894.7$ N/m^2
MTS	m^2	Sthene (sn) 1 sn = 1ton m/s^2 = 10^3 N	Pieze (pz) 1 pz = 10^3 N/m^2

1.4. CONVERSION FACTORS FOR VACUUM UNITS

Table 1.2

Interconversion of various vacuum units used in daily life practice

	Torr (mm Hg)	mbar	Micron	Nm^{-2} (Pascal)	Atmospheres
Torr (mm Hg)	1	1.33	10^3	133	1.32×10^{-3}
mbar	0.75	1	750	100	9.87×10^{-4}
micron (μ) Hg	10^{-3}	1.3×10^{-3}	1	0.133	1.32×10^{-6}
Nm^{-2} (Pascal)	7.5×10^{-3}	0.01	7.5	1	9.87×10^{-6}
Atmospheres	760	1.013	7.6×10^{-5}	1.01×10^5	1

1.5. REGIONS OF VACUUM AND THEIR CHARACTERISTICS

We speak of low, medium, high and ultra-high vacuum corresponding to the region of lower and lower pressure. These regions are distinguished from the point of view of the relationship in the kinetic theory of gases and according to the kind of gas flow.

Table 1.3:

Pressure Regions and Their Characteristics

Physical situation	**Rough**	**Medium**	**High**	**Ultrahigh**
Pressure [Torr]	760 – 1	$1 - 10^{-3}$	$10^{-3} - 10^{-7}$	$< 10^{-7}$
Particle number density [cm^{-3}]	10^{19} - 10^{16}	10^{16} - 10^{13}	10^{13} - 10^{9}	$< 10^{9}$
Mean free path [cm]	$< 10^{-2}$	10^{-2} - 10	$10 - 10^{3}$	$> 10^{3}$
Impingement rate [$cm^{-2} \times s^{-1}$]	$10^{23} - 10^{20}$	$10^{20} - 10^{17}$	$10^{17} - 10^{13}$	$< 10^{13}$
Collision frequency [$cm^{-3} \times$ s-1]	$10^{29} - 10^{23}$	$10^{23} - 10^{17}$	$10^{17} - 10^{9}$	$< 10^{9}$
Monolayer formation time [s]	$< 10^{-5}$	$10^{-5} - 10^{-2}$	$10^{-2} - 100$	> 100
Nature of gas flow	Laminar (Viscous)	Knudsen	Molecular	Molecular
Further special properties	Convection pressure dependent	Marked change of thermal conductivity of the gas	Transport phenomena proportional to pressure	Particles at surface >> particles in gas space

1.6. VACUUM PUMPS

The main purpose of vacuum pump is to reduce the gas density and, thereby, the gas pressure in a given volume. In terms of the working principle, vacuum pumps may be divided into two groups: (a) those which remove the gas particles from the pumped volume and discharge them to the atmosphere in one or more stages of compression. (b) Those which condense or in other manner (chemically) bind the particles to be removed at a solid wall, which is often a part of boundary of the volume being pumped.

Following are the major types of pumps according to their working principle.

(1) Mechanical pumps in which gas is trapped, compressed and removed from low pressure to high pressure side of the pump, where it is expelled to the atmosphere either directly or through second mechanical "backing" pump.

(2) Mechanical pumps which impart velocity to the pumped gas molecules by impact with swiftly moving solid surfaces. Such pumps are usually backed by another mechanical pump interposed between them and the atmosphere.

(3) Vapor-stream pumps in which the gas molecules to be pumped out are caused to move in the desired direction by impact with heavy molecules of pump fluid vapor, which derive their velocity by boiling from a liquid reservoir. With the exception of steam ejector pumps. A mechanical pump backs vapor-steam pumps.

(4) Chemical pumps in which the molecules to be removed from the workings chamber are caused to combine chemically with highly reactive substances (getter) such as titanium thus being converted to and trapped in the solid phase. The getters are generally dispersed on the pumps' surfaces by evaporator or by sputtering.

(5) Sorption pumps in which the molecules to be pumped out are physically sorbed (e.g. by Van der Waal forces) on specially prepared substances of large specific area (e.g. charcoal or zeolites). The sorption is aided by cooling the sorbent to below room temperature.

(6) Cryo-pumps are vessels with chemically non-reactive internal metal surfaces, cooled by refrigerants to condense the gases to be pumped.

In the pump types (1, 2, 3) the pumped gas is eliminated from the system, in other types it is retained.

1.7. VACUUM GAUGE

Vacuum gauge is a device which is used to measure the vacuum in a specified range. In any vacuum system, the most important parameter to be measured is gas pressure. There is not a single pump that can achieve the vacuum up to extreme ultra high vacuum range. Similarly, no gauge is available in the laboratory that can measure the vacuum of the whole spectrum. As different pumps produce vacuum of different degrees, in the same way, different gauges can

measure vacuum within specified ranges as per their design. Some of the gauges with their specified ranges are shown in the figure 1.2 [1,2].

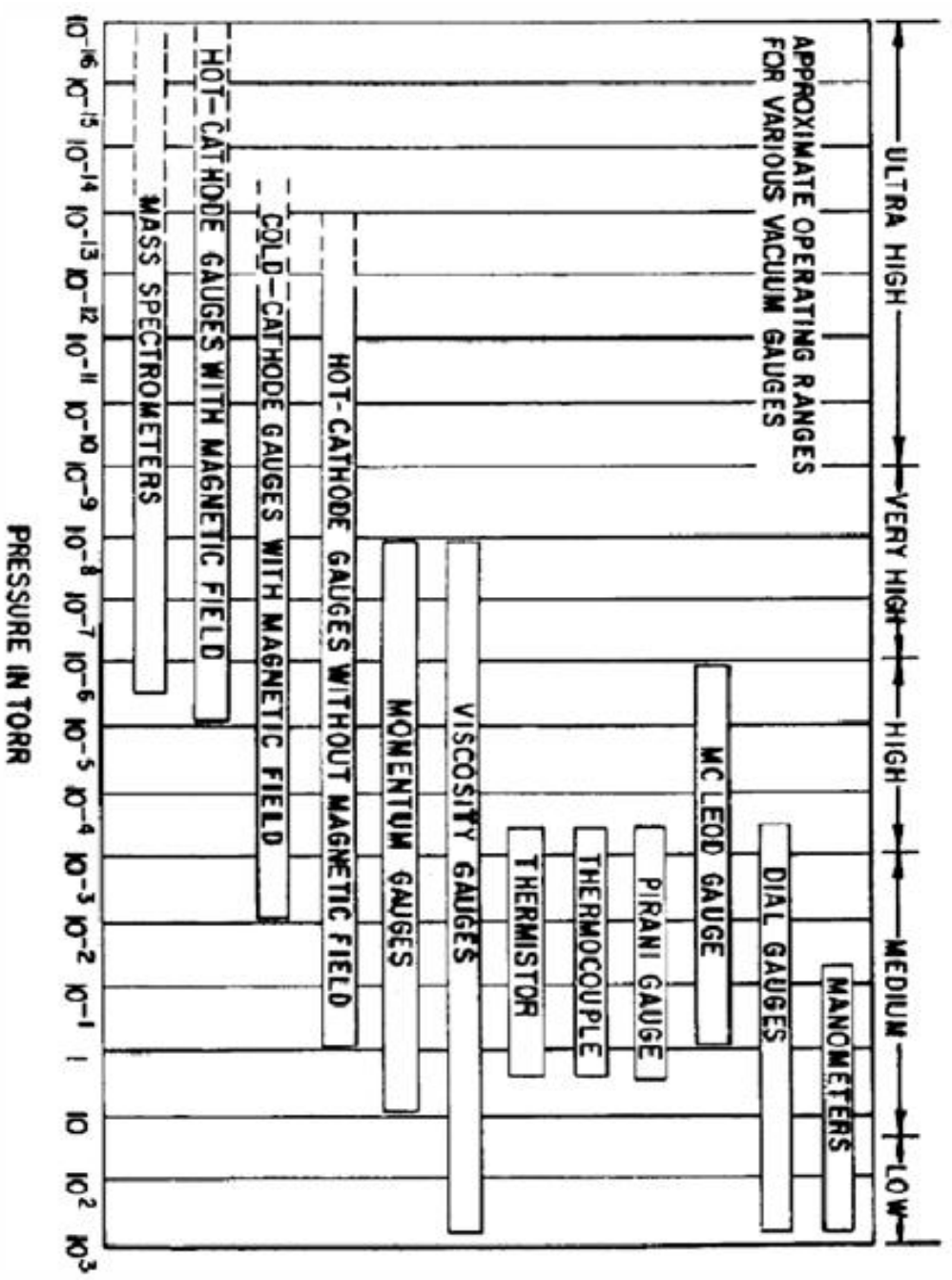

Figure 1.1: Classification of gauges and their working range of pressure according to their working principle

REFERENCES:

[1] Milton Ohring, The Materials Science of Thin Films, Academic Press, California (1992)

[2] S.W. Husain, Vacuum Science and Technology, Code No. 1718.

CHAPTER 2

INTRODUCTION TO THIN FILMS

Thin-film technology is simultaneously one of the oldest arts and one of the newest sciences. Involvement with thin films dates to the metal ages of antiquity [1]. Thin films are two dimensional materials deposited on a substrate, mainly of different materials. The limit, for which a film should be considered thin, is determined by thickness under which the anomalies behavior appears. In practice we consider the thin films between tenths of a nanometer and several micrometers [2]. It is not only the thickness that is important in defining a film, but rather the way it is created with the consequential effects on its microstructure and properties [3].

2.3. THIN FILM GROWTH MECHANISMS

Fabrication of thin films, involves the processes of nucleation and growth on the substrate or growth surfaces. The nucleation process plays a very important role in determining the crystallinity and microstructure of the resultant films. For the deposition of thin films with thickness in the nanometer region, the initial nucleation process is even more important. Nucleation in film formation is a heterogeneous nucleation. In practice, the interaction between film and substrate plays a very important role in determining the initial nucleation and the film growth. Many experimental observations revealed that there are three basic nucleation modes, as shown in the figure 1.1 and explained below [4].

(1) Island or Volmer-Weber growth
(2) Layer or Frank-van der Merwe growth
(3) Island-layer or Stranski-Krastonov growth

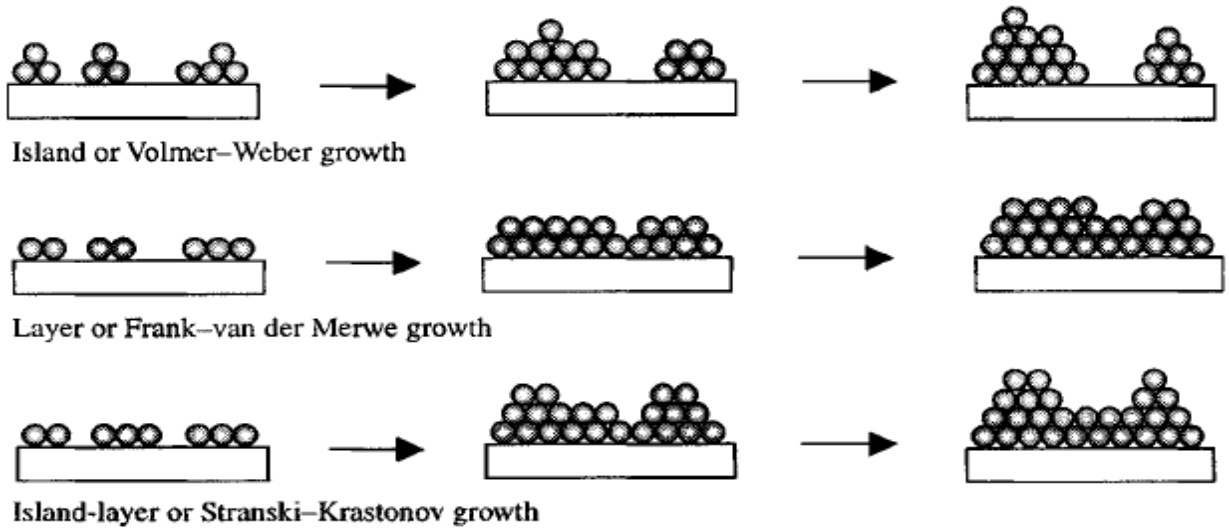

Figure 2.1: Thin Film growth mechanisms

2.3.1. ISLAND OR VOLMER-WEBER GROWTH

Island growth occurs when the growth species are more strongly bonded to each other than to the substrate. Many systems of metals on insulator substrates, alkali halides, graphite and mica substrates display this type of nucleation during the initial film deposition. Subsequent growth results in the islands to coalesce to form a continuous film.

2.3.2. LAYER OR FRANK-VAN DER MERWE GROWTH

The layer growth is the opposite of the island growth, where growth species are equally bound more strongly to the substrate than to each other. First complete monolayer is formed, before the deposition of second layer occurs. The most important examples of layer growth mode are the epitaxial growth of single crystal films.

2.3.3. ISLAND-LAYER OR STRANSKI-KRASTONOV GROWTH

The island-layer growth is an intermediate combination of layer growth and island growth. Such a growth mode typically involves the stress, which **is** developed during the formation of the nuclei or films.

2.4. THIN FILM DEPOSITION TECHNIQUES

Deposition technique and its associated process parameters have a characteristic effect on the nucleation and growth-dominated microstructure of a tin film and its physical properties [3]. There are many techniques to prepare thin films. Each technique has advantages and

disadvantages which must be optimized to yield desirable properties. These deposition techniques may broadly be divided as follows [1-4]:

1. Physical Vapor Deposition (PVD)
2. Chemical Vapor Deposition (CVD)
3. Electrolyses or Solution Growth
4. Electro-Chemical Deposition (ECD)

We will be concentrating on PVD and specifically on Thermal evaporation.

2.4.1. PHYSICAL VAPOR DEPOSITION (PVD)

PVD is a process of transferring growth species from a source or target and deposit them on a substrate to form a film. The process proceeds atomistically and mostly involves no chemical reactions. Various methods have been developed for the removal of growth species from the source or target. The thickness of the deposits can vary from angstroms to millimeters.

In general, those methods can be divided into two groups:

(1) Sputtering

(2) Evaporation

2.4.1.1. SPUTTERING

Sputtering relies on a plasma (usually a noble gas, such as Argon) to knock material from a target a few atoms at a time. The target can be kept at a relatively low temperature, since the process is not one of evaporation, making this one of the most flexible deposition techniques. It is especially useful for compounds or mixtures, where different components would otherwise tend to evaporate at different rates [5].

2.4.1.2. EVAPORATION

It is a known fact that atoms or molecules are librated by heating from every material in its solid or liquid phase and that in a closed system a certain equilibrium pressure, which is called the saturated vapor pressure is established at a given temperature.

The number of particles with molecular weight M evaporated at a temperature T (at equilibrium) per unit time from clean surface of unit area using elementary kinetic theory is given by [6]:

$$N_e = 3.513 \times 10^{22} \frac{P_e}{\sqrt{M\,T}} \qquad \text{Molecules cm}^{-2}\ \text{s}^{-1}$$

Where P_e is the equilibrium vapor pressure (in torr)

If the system is not in equilibrium and there is relatively lower temperature in some part of it, the vapor will condense in this part and conditions will thus be established for a transfer of material from evaporation source to a colder substrate. The deposition of a film by evaporation is thus essentially a non-equilibrium process.

The librated particles travel in space with their thermal velocities along the straight path until they collide with atoms of residual gas. To ensure a straight path for them between the source and substrate, the space must be sufficiently exhausted, in order to provide the larger mean free path [1-4].

2.4.1.2.1. VAPOR SOURCES

The evaporation of the materials in a vacuum system requires a vapor and to supply the heat of vaporization while maintaining the charge at a temperature sufficiently high to produce the desired vapor pressure.

- A thermal evaporator uses an electric resistance heater to melt the material and raise its vapor pressure to a useful range. This is done in a high vacuum, both to allow vapor to reach the substrate without reacting with or scattering against other gas-phase atoms in the chamber, and reduce the incorporation of impurities from the residual gas in the vacuum chamber.
- An electron beam evaporator fires a high-energy beam from an electron gun to boil a small spot of material; since the heating is not uniform, lower vapor pressure materials can be deposited.
- Pulsed laser deposition systems work by an ablation process. Pulses of focused laser light vaporize the surface of the target material and convert it to plasma. This plasma usually reverts to a gas before it reaches the substrate [5].

2.4.1.3. RESISTIVE HEATING

The temperature of the materials for evaporation may be raised by direct or indirect heating. To avoid contamination of the deposit, the support materials itself have negligible vapor and dissociation pressure at the operating temperature. Suitable materials are refractory metals (W, Mo, Ta) and oxides. The most desired sources are availaboratoryle in the shapes of wire, boat sheet and crucibles according to requirements [1, 6]. The simple vapor sources are resistance-heated wires and metal foils of various types made of refractory metals.

2.4.1.4. CLOSE SPACE SUBLIMATION (CSS)

Close Space Sublimation is a type of thermal evaporation and detailed description about CSS will be discussed in the chapter 4. In the present research, we have employed CSS technique for the fabrication of Cadmium Sulfide thin films. The CSS process offers the advantage of simplified deposition and high transport efficiency conducted under low vacuum conditions at moderate temperatures.

In CSS, source material is placed in powder form in a graphite boat which is being heated by electric lambs. The material starts to sublime and deposit on the substrate placed in a mica sheet, which acts as a thermal insulator between the source and the substrate. The source is maintained at higher temperature than substrate. The deposited film presents a high crystallographic orientation and adequate opto-electrical properties for photovoltaic applications.

REFERENCES:

[1] M. Ohring, *The* Materials Science, of Thin Films, **Academic** Press, San Diego, New York, Boston, London, Sydney, Tokyo, Toronto, (1992).

[2] L. Eckertova, Physics of Thin Films, Plenum Press, New York, (1977).

[3] K. L. Chopra and S. R. Das, Thin Film Solar Cells, Plenum Press, New York (1983).

[4] G. Cao, NanoStructures and NanoMaterials, Imperial College Press, (2004).

[5] A. Ali, "Fabrication and Characterization of two sourced evaporated Cd-based II-VI thin films"

[6] Z. Ali, Fabrication of II-VI Semiconductor Thin Films and a Study of Structural, Optical and Electrical Properties, Ph.D. Thesis, Quaid-i-Azam University, 2005

CHAPTER 3

CADMIUM SULFIDE THIN FILMS AND THEIR PROPERTIES

INTRODUCTION

Binary and ternary compounds present wide range of optical and electrical properties. These properties make them an important class of materials and competing candidates for silicon and other semiconductor materials in photovoltaic and optoelectronic applications [1].

3.6. PROPERTIES AND STRUCTURE OF CdS

Cadmium Sulfide is II-VI compound semiconductor and yellow in color. Table 2-1 [7,8] shows the Basic properties of cadmium sulfide.

Table 3.1:

Basic properties of cadmium sulfide

Formula as Commonly Written	CdS			
Synonyms	cadmium orange			
Hill System Formula	Cd_1S_1			
Molecular Weight	144.477			
Colour	yellow to orange			
Appearance	crystalline solid			
Melting Point	1750°C			
Boiling Point °C	980 °C Sublimes			
Density	4.830 g cm^{-3}			
Specific Gravity	4.830			
Electronic Configuration	Element	%	Formal oxidation state	Formal electronic configuration
	Cd	77.81	2	$[Kr].4d^{10}$
	S	22.19	-2	$[Ne].3s^2.3p^6$
Solubility in Water	insoluble			

3.7. FABRICATION TECHNIQUES OF CdS THIN FILMS

CdS thin films have been deposited by several techniques, including chemical bath deposition [9], thermal evaporation [10], electrochemical deposition [11], spray pyrolysis [12, 13], laser ablation [14], electron beam evaporation [15] and closed space sublimation [16].

In the Present work, we have deposited CdS thin films by close space sublimation (CSS) technique which will be explained in chapter 5.

3.8. STRUCTURAL PROPERTIES OF CdS THIN FILMS

Different studies have been shown that CdS exists in both hexagonal (wurtzite) [3] and cubic (zinc blend) [4] phases as shown in Figure 2-1. The formation of cubic or hexagonal phase or mixed structure of the two depends on many factors including the deposition technique. The hexagonal structure is the stable phase of CdS at room temperature and later is found at higher temperature [17].

Zinc blende structure is two interpenetrating FCC sub-lattices composed of entirely different atoms. In case of CdS, these atoms are Cd and S, as shown in the figure 2-1 [7].

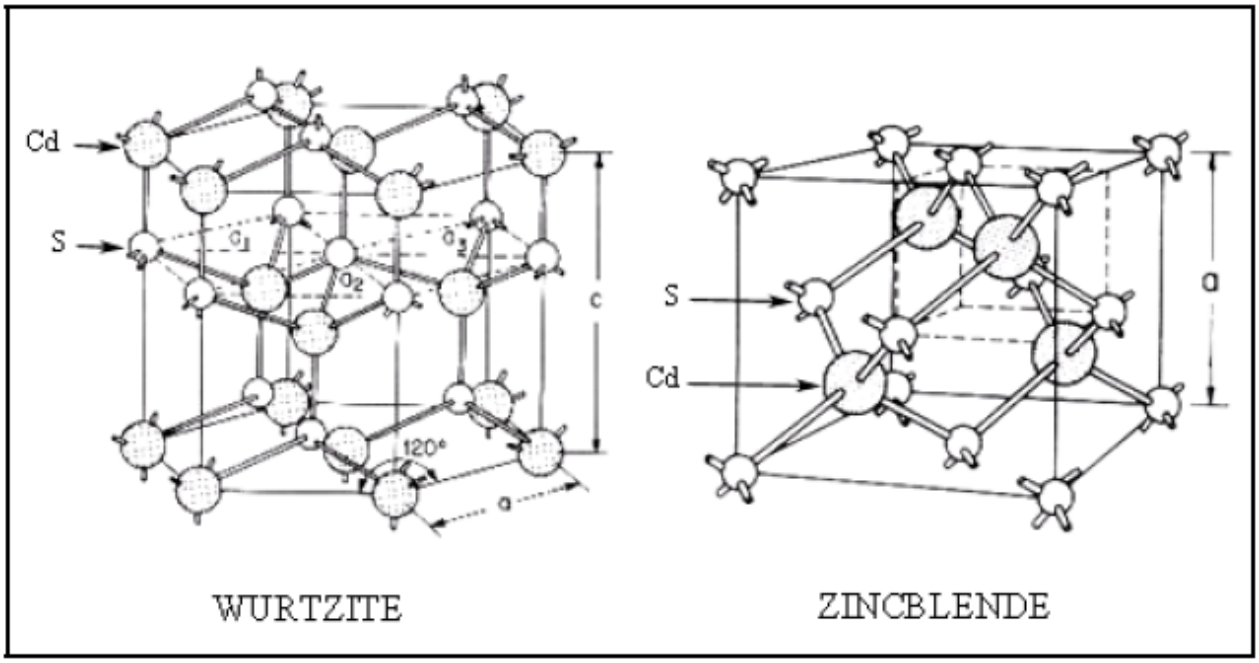

Figure 3.1: Hexagonal (Wurtzite) and Cubic (Zincblende) structures of CdS

Enriquez *et al.* [18] reported that the lattice parameters, grain size and the strain have a direct dependence on the film thickness. They found that when the thickness increases the grain size increases where as the strain decreases. It was also observed that the peak intensity in the diffraction patterns increases as the film thickness increase and the lattice parameters *a* and *c* values of the strain-free samples are respectively 4.16 and 6.756 Å.

3.9. OPTICAL PROPERTIES OF CdS THIN FILMS

CdS has a band gap of 2.45eV [2]. The wavelength corresponding to the band gap energy is approximately 512 nm, green, i.e. in the visible range of the electromagnetic spectrum. Bright sunlight provides an irradiance of just over 1 kilowatt per square meter at sea level. Of this energy, 527 watts is infrared radiation, 445 watts is visible light, and 32 watts is ultraviolet radiation [19], which shows that relatively more energy can be achieved by using a photo-device which is more sensible to infrared and visible regions of light. CdS thin films as window layer application in solar cells perform exactly the same operation. It absorbs the ultraviolet and becomes transparent window for visible and infrared regions of light. Due to high band gap, it has a potential application in thin film solar cells as a window layer material. CdS can also be used for making light emitting diodes (LED) and lasers [5].

3.10. ELECTRICAL PROPERTIES OF CdS THIN FILMS

CdS thin films grow as n-type semiconductor due to the donor centers formed during deposition. Vacancies of sulfur cause deviations from stoichiometry. However, by means of thermal diffusion of impurities, such as Cu and In, after preparation, it is possible to obtain p-type CdS [6]. The Cd:S ratio during evaporation sensitively influences the electrical properties as does doping. For In-doped CdS films, the best electrical properties are obtained at a Cd:S ratio of 1.5 at which the films also exhibit the best structural characteristics. Resistivity values as low as 10^{-3} Ω cm have been obtained on CdS:In (1.5%) samples [17].

REFERENCES:

[1] Z. Ali, Fabrication of II-VI Semiconductor Thin Films and a Study of Structural, Optical and Electrical Properties, Ph.D. Thesis, Quaid-i-Azam University, (2005).

[2] Moons, D. Gal, J. Beier, G. Hodes, D. Cahen, L. Kronik, L. Burstein, B. Mishori, Y. Shapira, D. Hariskos, M. Schock, Sol. Energy Mat. Sol. Cells 43 _1996. 73.

[3] E. Wiberg, A.F. Holleman, *Inorganic Chemistry*, Elsevier, (2001). CRYSTALLINE CADMIUM SULFIDE, MS Thesis, Green State University, 2007.

[4] R. J. Traill, R. W. Boyle Hawleyite, isometric cadmium sulphide, a new mineral. *American Mineralogist* 40, (1955).

[5] M. Bhowmick, INVESTIGATION OF OPTOELECTRONIC PROPERTIES IN THIN-FILM AND CRYSTALLINE CADMIUM SULFIDE, MS Thesis, Green State University,2007

6] A. Romeo, D. L. Batzner, H. Zogg, C. Vignali and A. N. Tiwari, Solar Energy Materials & Solar Cells, 67 (2001) 311-221.

[7] A.S. AL-SHAMMARI, PREPARATION AND CHARACTERIZATION OF CHLORINE DOPED CADMIUM SULPHIDE THIN FILMS AND THEIR APPLICATIONS IN SOLAR CELLS, MS Thesis, King Saud University, (2005)

[8] http://en.wikipedia.org/wiki/Cadmium_sulfide

[9] L.M. Fraas, W.P. Bleha and P. Braatz, Appl. Phys. 46(1947) 491.

[10] A. Shours, N. Elkadry, and N. Mahmoud, Thin Solid Films 269 (1975) 117.

[11] D.P. Amalnerkar, K. Yamaguchi, T. Kajita and H. Minoura, Solid State Commun. 90(1994)3.

[12] S. Mathew, P.S. Mukerjee and K.P. Vijaykumar, Thin Solid Films 254 (1995) 278.

[13] J. Ebothe, J. Appl. Phys. 77 (1995) 232.

[14] S. Keitoku, H. Ezumi, H. Osono and N. Ohto, Apn. J. Appl. Phys. 34 (1995)L138.

[15] J. G. Werthn, A.L. Fahrebruch, R.H. Bube and J. C. Sesch, J. Appl. Phys. 54 (1993) 2750.

[16] D. Albin, D. Rose, R. Dhere, D. Levi, L. Woods, a. Swartzlander, And P. Sheldon, 26th IEEE Photovoltaic Specialists Conf. 1997, Anaheim, California.

[17] K. L. Chopra and S. R. Das, Thin Film Solar Cells, Plenum Press, New York (1983).

[18] J. P. Enriquez and X. Mathew, Solar Energy Materials & Solar Cells 76 (2003) 313-322

[19] Solar Spectral Irradiance: Air Mass 1.5, http://rredc.nrel.gov/solar/spectra/am1.5/. Retrieved 2009-11-12.

CHAPTER 4

CHARACTERIZATION TECHNIQUES

This chapter will address the experimental techniques and applications associated with determination of

1. Morphological Properties Elemental Composition
2. Structural Properties
3. Optical Properties
4. Electrical Properties

Scanning Electron Microscope (SEM) was used to determinte the morphology and Energy Dispersive X-rays (EDX) installed within SEM for elemental composition. Structural analysis was done by X-Ray Diffraction (XRD). Spectrophotometer was used to determine the optical constants (refractive index, film thickness, energy gap etc). The electrical properties (resistivity, career concentration, careers type etc) were measured by Ecopia Hall apparatus. A short description of each technique is given below.

4.5. MORPHOLOGICAL AND ELEMENTAL COMPOSITIONAL CHARACTERIZATIONS

In semiconductor thin films, morphology of films is very important to note. It directly gives the influence on optical and electrical properties. EDX is important to see is there any element as an impurity except required.

4.5.1. SCANNING ELECTRON MICROSCOPE (SEM & EDX)

SEM is a basic tool for material characterization especially microstructural/morphological properties. It can provide important information about the surface features of an object, its texture, the shape, size and arrangement of the particles making up the object that are lying on the surface of the sample, the elements and compounds the sample is composed of and their relative ratios in areas ~ 1 μm in diameter. Scanning electron microscope resolutions are

currently limited to around 25 Angstroms. Figure 4.1 shows a schematic diagram of scanning electron microscopy

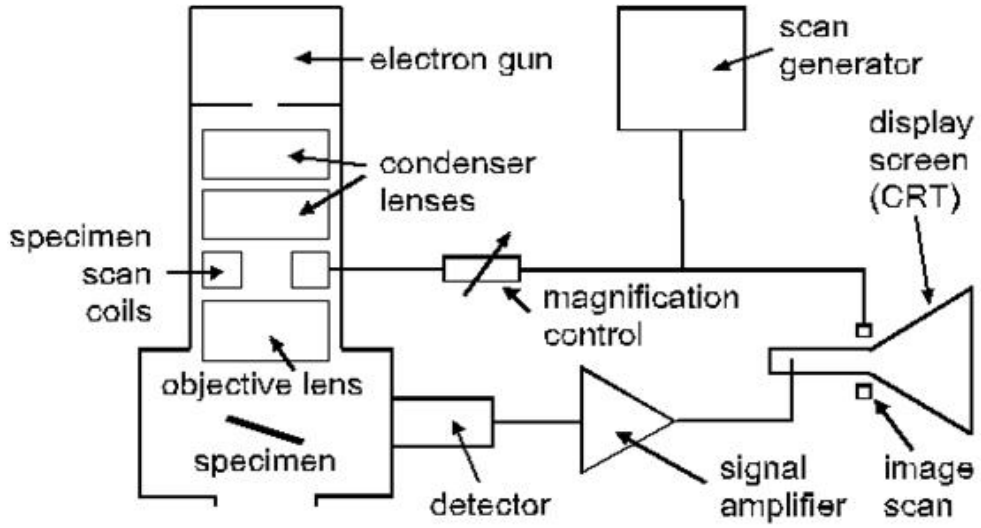

Figure 4.1: Schematic Diagram of SEM

The scanning electron microscope generates a beam of electrons in a vacuum. This beam is collimated by electromagnetic condenser lenses, focused by an objective lens and scanned across the surface of the sample by electromagnetic deflection coils. The primary imaging method is by collecting secondary electrons that are released by the sample. The secondary electrons are detected by a scintillation material that produces flashes of light from the electrons. The light flashes are then detected and amplified by a photomultiplier tube hence; an image is formed that is strikingly similar to what would be seen through an optical microscope.

Backscatter imaging uses high energy electrons that emerge nearly 180 degrees from the illuminating beam direction. The backscatter electron yield is a function of the average atomic number of each point on the sample, and thus can give compositional information. Scanning electron microscopes are often coupled with x-ray analyzers. The energetic electron beam - sample interactions generate x-rays that are characteristic of the elements present in the sample [6]. Two types of detectors are used: energy-dispersive x-rays (EDX) and wave-dispersive x-rays (WDX). EDX is commonly used for rapid sample analysis and for spatial map of individual elements. It is particularly insensitive to light elements in heavy matrix [2]. It is well suited for quantitative measures of metals on semiconductors, alloy compositions and so on. Detection of carbon, oxygen and nitrogen is difficult because of low x-ray yield. The most important

technique for quantifying results is called ZAF; ZAF is acronym from three separate effects, atomic number (Z), absorption (A) and fluorescence (F) which the method compensates for [5].

The micrograph of the thin films and EDX were carried out in jeol Scanning Electron Microscope system with EDX attached to it. To reduce the charging effect of electrons (causing image defects) on the film surface due to high resistivity of films, a thin gold layer of 200Å was coated by Jeol Ion Sputtering coater. With ZAF method the relative quantitative (Z>11) of 1-10% could be achieved.

4.6. STRUCTURAL CHARACTERIZATIONS

The determination of crystal structure is important in solid state physics especially in the case of semiconductors. These structural properties usually influence the physical properties of solids.

4.6.1. X-RAY DIFFRACTION

X-ray diffraction technique is the most suitable, non-destructive and most precise method for crystal structure analysis. It is simple because no elaboratoryorated sample preparation is required [1,2]. A monochromatic beam of x-ray that falls upon a crystal is scattered in all direction within it, but owing to the regular arrangement of the atoms, in certain directions the scatted waves constructively interfere with one another while in others they interfere destructively. Constructive interference taken place only between those scattered rays which satisfy the Bragg's law:

$$\lambda = 2\, d\, \mathrm{Sin}\theta \qquad (4.1)$$

Where, λ is the wavelength of the X-ray beam incident upon a crystal at angle θ with the family of planes whose spacing is d.

In case of the rotating-crystal method, a crystal is mounted with one of its axes, or some important crystallographic directions, normal to monochromatic x-ray beam. As crystal rotates a particular se of lattice planes will make correct Bragg's angle for reflection of the monochromatic incident beam [3]. Improved detection methods for x-rays, the availaboratoryility of commercial monochromators, and intense micro-focus x-ray sources have made XRD method applicable to films as thin as 50 Å. The method is generally applied to films

thickness of several hundred Å [4,5]. Analysis of diffraction pattern obtained and comparison with standard ASTM data can reveal the existence of different crystallographic phases, their relative abundance, the lattice parameters and any preferred orientations in the film [1].

4.6.1.1. DETERMINATION OF THE CRYSTALLITE SIZE

We can estimate the particle size of very small crystals from their diffraction curves by taking the width of these curves and using the relation [3].

$$t = \frac{\lambda}{\beta \cos\theta_\beta} \qquad (4.2)$$

Where, β is the width at the half maximum intensity measured in radians as shown in Figure 4.2 and λ is wavelength. In the present work CuK_α (λ = 1.5418 Å) radiations were used for the experiments and the measurements were made at room temperature.

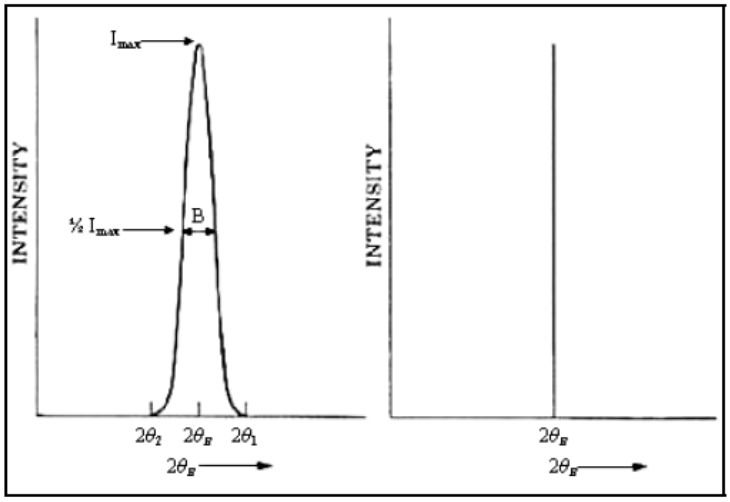

Fig. 4.2: The using of diffraction curve to determine the particle size.

XRD pattern were obtained by STOE X-Ray Diffraction machine and crystal Structure with phase analysis were carried out on the software STOE installed on the computer attached with XRD machine.

4.7. OPTICAL CHARACTERIZATION

Optical characterization of thin film includes transmittance, refractive index, reflectance, absorption coefficient, and band gap. The reflection, transmission and interferometric properties

of thin films have made it possible to determine the optical constants conveniently [1]. The absorption studies have led to a variety of interesting thin film optical phenomena which have thrown considerable light on the electronic structure of solids. The films are characterized by refractive index (n).

Energy gaps (E_g) are of two types in semiconductors [1].

1. Direct energy gap
2. Indirect energy gap

1. For a semiconductor in which the minimum of the conduction band and maximum of the valance band occurs at the same value of k, absorption begins at $h\nu = E_g$ and electrons are transferred vertically between the two bands without a change in momentum, it is called directenergy gaps. II-VI group compounds are of this type of energy gap.
2. In semiconductors where the conduction band minima and the valance band maxima occur at different k values, optical transitions from the valance band to the conduction band require the participation of phonons in order to conserve momentum because of the change in the electron wave vector. Phonon is either emitted or absorbed.

Transmission or transmittance of a film is the only property, which is obtained directly from the film, rest are inferred from the transmission spectra. Transmission spectra of the samples were recorded on UV-VIS/NIR spectrophotometer (Perkin Elmer Lambda 900), interfaced with a computer by UV-WinLaboratory software. Transmission is plotted versus wavelength as shown in the figure 4.3. Refractive index and thickness of films are measure with the help following formulas:

The refractive index (n) is measure by following formula.

$$n = \frac{[N + (N^2 - 4s^2)^{\frac{1}{2}}]}{2} \qquad (4.3)$$

Where,

$$N = 1 + s^2 + 4s\left(\frac{T_{max} - T_{min}}{T_{max} * T_{min}}\right) \qquad (4.4)$$

In above equations, s is the refractive index of glass (s = 1.52), T_{max} is the maximum transmission and T_{min} is very next minimum transmission as shown in the figure 4.3.

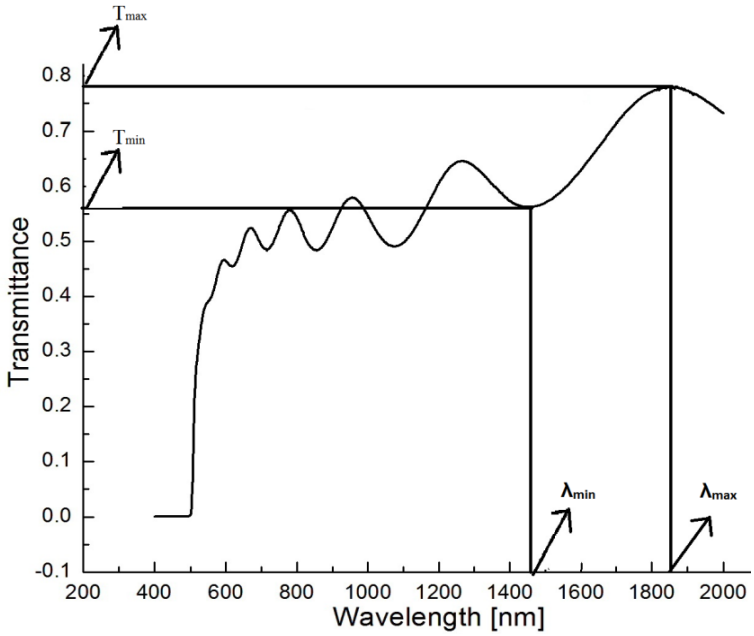

Figure 4.3: Transmission spectrum to measure the thickness and refractive index

Thickness of the film is determined from the formula:

$$\frac{\lambda_{max}\lambda_{min}}{4n(\lambda_{max}-\lambda_{min})} \qquad (4.5)$$

λmax, λmin are the values of wavelengths corresponding to maximum and minimum transmission respectively as shown in the figure 4.3.

4.8. ELECTRICAL PROPERTIES

The Hall Effect and the electrical resistivity are the key parameters used in investigations of the basic electrical conduction processes in semiconductor materials.

4.8.1. HALL EFFECT

Hall Effect is phenomena of producing potential difference across an electrical conductor in the presence of magnetic field. This potential difference is known as Hall voltage. The direction of this hall voltage is perpendicular to both current and magnetic field as shown in Figure 4.4.

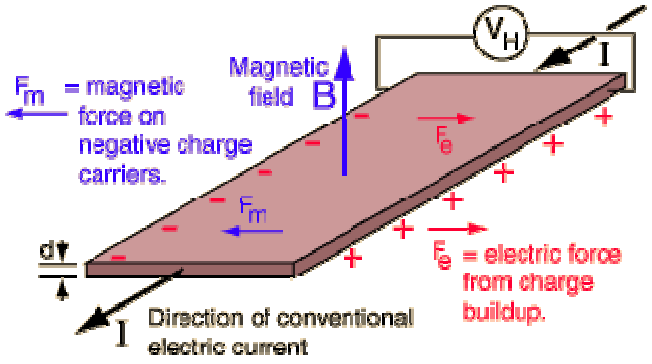

Figure 4.4: The schematic diagram showing Hall voltage across the sides of conductor in presence of magnetic field.

The mathematical expression **for Hall voltage** is given by equation

$$V_H = \frac{-IB}{dne} \qquad (4.6)$$

Where I is current across the conducting plate, B is magnetic field, d is depth of the plate, e is electron charge and n is charge carrier density (number of charge carriers per unit volume).

Simple **hall coefficient, R_H** can be calculated from equation 4.7

$$R_H = \frac{E_y}{j_x B} = \frac{dV_H}{IB} = -\frac{1}{ne} \qquad (4.7)$$

The important facts discovered after the idea of Hall Effect were:

- Hall Effect differentiated between positive charges moving in one direction from negative charges moving in other.
- it provided us the ideas that electric current in metals is carried by electrons not by protons
- In some substances such as semiconductors, it was more appropriate to think of the current as holes moving rather than electrons.
- With the help of Hall Effect, we can measure different parameters, Hall mobility and doping type of the material.

Hall mobility (μ) is defined as the product of hall coefficient (R_H) and the conductivity (σ).

$$\mu = R_H \ \sigma \qquad (4.8)$$

The mathematical expression for Hall coefficient is defined above, whereas conductivity is an inverse of Resistivity (ρ). Resistivity is given by Equation 4.9.

$$\rho = R\frac{A}{l} \qquad (4.9)$$

Where R is electrical resistance, A is area, and l is length of the samples.

The **doping type** of the material (p-type or n-type) can also be tested by Hall Effect. This is tested by the sign of the Hall voltage, if it positive the material is p-type and if the sign is negative the material is n-type.

4.8.2. ELECTRICAL RESISTIVITY

The resistance (R) of rectangular shape (fig 4.5) of thin film (measured in direction parallel to the film surface) at constant temperature is given by,

$$R = \frac{\rho}{d}\frac{l}{b} \qquad (4.10)$$

Figure 4.5

Where ρ is the resistivity, d is the thickness *l* and b are the length and width of the rectangular shape film.

The most commonly used method for measuring the resistivity of arbitrary shaped sample is known as Vander Pauw method [2]. The specific resistivity of a flat sample of arbitrary shaped can be measured without knowing the current pattern, if the following conditions are met:

(1) The contacts are at the circumference of the sample
(2) The contacts are sufficiently small
(3) The sample is uniformly thick and the surface of the sample is singly connected, i.e. the sample does not contain any isolated holes.

Considering a flat sample of a conducting material of arbitrary shape, with contacts 1,2,3 and 4 along the periphery to satisfy the conditions discussed. The resistance $R_{12,34}$ is defined as:

$$R_{12,34} = \frac{V_{34}}{I_{12}} \qquad (4.11)$$

Where the current I_{12} enters the sample through the contact 1 and leaved through contact 2 and $V_{34} = V_3 - V_4$ is the voltage difference between the contact 3 and 4; $R_{23,42}$ is defined similarly. The resistivity is given by [2]:

$$\rho = \frac{\pi t}{\ln(2)} \frac{(R_{12,34} + R_{23,41})}{2} F \qquad (4.12)$$

For symmetrical sample such as circular or square F = 1.

4.8.3. HALL MEASUREMENTS BY ECOPIA HMS-3000

ECOPIA HMS-3000 was used to measure resistivity, carries concentration, career type, hall coefficient and mobility of CdS thin films. The CdS thin films were cut in 6 x6 mm size. Silver paste was dropped on four corners to make contacts. After the paste had dried the film was put in the PCB holder and the spring clips were put exactly on the silver paste points, as shown in the figure 4.6. PCB holder with thin film sample was mounted in a dark funnel. The measurements were taken at room temperature (300 K). This whole setup was configured with computer; resistivity and hall parameters were noted from monitor screen.

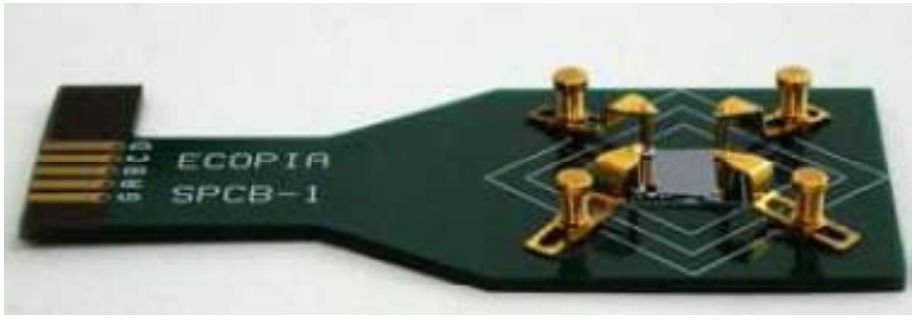

Figure 4.6: PCB with a thin film sample to measure its resistivity and hall parameters

REFERENCES:

[1] K. L. Chopra and S. R. Das, Thin Film Solar Cells, Plenum Press, New York (1983).

[2] D. K. Schroder, Semiconductor materials and Device Characterization (2nd Edition), A Wiley-Interscience publication, John Wiley & Sons, Inc., (1998).

[3] B.D. Cullity, Element of X-Ray Diffraction, Addison-Wesley publishing Company, Inc. (1978)

[4] K. L. Chopra, Thin Film Phenomena, McGraw-Hill book Company, NY, (1969

[5] L. Eckertova, Physics of Thin Films, Plenum Press, New York, (1977).

[6] www.unl.edu/CMRAcfem/semoptic.htm.

[7] G. Lawes. A. M. James, Scanning Electron Microscope and X-Ray Microanalysis. John Wiley & Sons, Chichester (1987).

CHAPTER 5

DESIGN AND ASSEMBLY OF CLOSE SPACE SUBLIMATION EQUIPMENT

INTRODUCTION

Close Space Sublimation (CSS) process offers the advantage of simplified deposition and high transport rate under low vacuum conditions at moderate temperatures [1]. In CSS technique, films are deposited by sublimation of the source material and condensation of the resulting vapors on the substrate which is placed close to source. This whole process is conducted in vacuum. Therefore chapter 1 discussed briefly about vacuum science and technology.

5.1. THEORY

Sublimation describes the direct phase transition between a solid and gas state. A close Space sublimation deposition is dependent on following [2].

- The sublimation process at the surface of the source,
- The transport of the gas from the source to the substrate surface,
- The sublimation process at the surface of the substrate

In this technique, the substrate is placed just above a CdS source in closed vicinity. Source and Substrate are then heated simultaneously by an external source, maintaining a constant temperature difference between the two. The deposition is carried out in vacuum environment.

The main advantage of CSS over other processes is its high deposition rate. Based on a detailed investigation of close space sublimation, it is found that the material transport and hence the growth depend on (1) the spacing between the source and substrate, (2) source and substrate temperature, (3) ambient pressure, (4) composition of the source material [3].

5.1.1. THE SPACING BETWEEN THE SOURCE AND SUBSTRATE

The spacing between the source and the substrate has to be an optimum affordable minimum. This would not only increase the deposition rate but also reduce the material consumption per

deposition. It is desirable that nearly all the material consumed for the source is deposited on the substrate. The growth rate varies inversely as the spacing [4].

5.1.2. SOURCE AND SUBSTRATE TEMPERATURE

Work by Nagayoshi and Suzuki [5] observed that the deposition rate increased as the source temperature increased for a deposition under vacuum, in agreement with a sublimation limited case. An increase in substrate temperature leads to a decrease in the resistivity. The grain size of film appears to increase with increasing substrate temperature. One should expect, since the surface mobility of the depositing species increases leading to less nucleation sites and therefore larger grains [6].

5.1.3. AMBIENT PRESSURE

In vacuum, transportation of molecules from source to substrate is significantly enhanced and larger growth rates were obtained due to larger mean free path available as compared to the situation when a gas is filled in the deposition chamber.

Vacuum is important for two reasons [7].

- It is possible to grow relatively thick films in a vacuum environment, without making an excessive number of cycles.
- The films can be grown at lower temperatures than those required when using an inert gas environment with the subsequent advantage of decreasing inter-diffusion processes.

5.1.4. COMPOSITION OF THE SOURCE MATERIAL

Material to be deposited, (CdS 99.99% pure in our case) must be in pure and powder form. Pure and small particle sized powder of material is sublimated at low temperature as compared to agglomerated and impure powder.

5.2. DEVELOPMENT OF CSS UNIT

CSS unit for the fabrication of thin films was built and installed at TT Laboratory, SCME, NUST, Islamabad. Although technique is internationally available in the literature but the beauty of this CSS unit installed is that it has been made of the accessories which are available in local market.

5.2.1. SELECTION OF MATERIAL

Keeping in view, the various properties (cost, welding, machining, out gassing, corrosion etc.), we choose Stainless Steel 304-Low carbon (SS304-L) for chamber construction. This was originally called 18-8 which stood for its chromium and nickel content [8]. It is the most versatile and most widely used stainless steel, available in a wider range of products, forms and finishes than any other. Grade 304 also has outstanding welding characteristics. Grade 304L, the low carbon version of 304, does not require post-weld annealing and so is extensively used in heavy gauge components (over about 6mm) [9]. Elemental Composition of SS304 is shown in the Table 5.1.

Table 5.1:
Elemental composition of ss304

Grade		C	Mn	Si	P	S	Cr	Mo	Ni	N
304	min.	-	-	-	-	-	18.0	-	8.0	-
	max.	0.08	2.0	0.75	0.045	0.030	20.0		10.5	0.10
304L	min.	-	-	-	-	-	18.0	-	8.0	-
	max.	0.030	2.0	0.75	0.045	0.030	20.0		12.0	0.10
304H	min.	0.04	-	-	-0.045	-	18.0	-	8.0	-
	max.	0.10	2.0	0.75		0.030	20.0		10.5	

5.2.2. LIST OF ACCESSORIES USED IN CSS COATING UNIT

1. Cylindrical Jar
2. Flange (base plate)
3. Three Steel rods
4. Supporting plate
5. Graphite Boat (material holder)
6. Mica Substrate holder
7. Graphite Slab
8. Heating Assembly (lambs, thermo couples, temperature controllers)
9. Vacuum Assembly (Rotary Pump and Pirani Gauge)

The vacuum chamber as shown in the figure 5.1, built for this research is consisted of a vertical jar. Stainless Steel sheet of wall thickness 2mm was used to construct this vacuum jar. The height of this jar is 300mm and internal diameter is 288mm. Three glass windows of internal diameter 100mm were made to observe the internal situation of the chamber. Stainless Steel shutter were fitted in front of windows to avoid them from continues exposure of light, so the glass may not break. A smooth rim of internal diameter equal to the jar diameter and external diameter of 330mm was welded at the base of jar to keep the jar airtight with the base plate (flange) in the presence of an O-ring, to sustain vacuum inside the chamber

Figure 5.1: Photo of the CSS equipment built in this project

A circular flange, shown in the figure 5.3., has a diameter 330mm with some feed throughs (for vacuum pump, electrical wires and thermocouple) was used to mount the other assembly on it. Three rods of diameter 12.50mm and height of 250mm were fitted vertically on the flange. Supporting steel was fitted on rods to mount source, substrate and heating lambs. A graphite boat of depth 11mm, base thickness 3mm, length 50mm and width of 25mm was used to hold the source material. Two halogen lambs 1000Watts and 500Watts are used to heat source material placed in graphite boat and substrate placed in mica frame, covered with a graphite slab respectively. Graphite slab is used to heat the substrate gently and uniformly. Mica acts as a thermal insulator between source and substrate. Two K-type thermo-couples are inserted in the graphite slab and graphite boat to read the temperature of source and substrate. Other ends of the thermo-couples are fed to two proportional integral derivative (PID) temperature controllers (Swiftch, SG-632), one for source and other for substrate. These controllers vary their output depending on the difference between a measured temperature of the chamber and a set point temperature. The controllers have a `SMART' algorithm which adjusts the parameters of the controllers to improve the effectiveness of the control. Two magnetic relays are used to turn lamps on and off according to the sequence received from temperature controllers

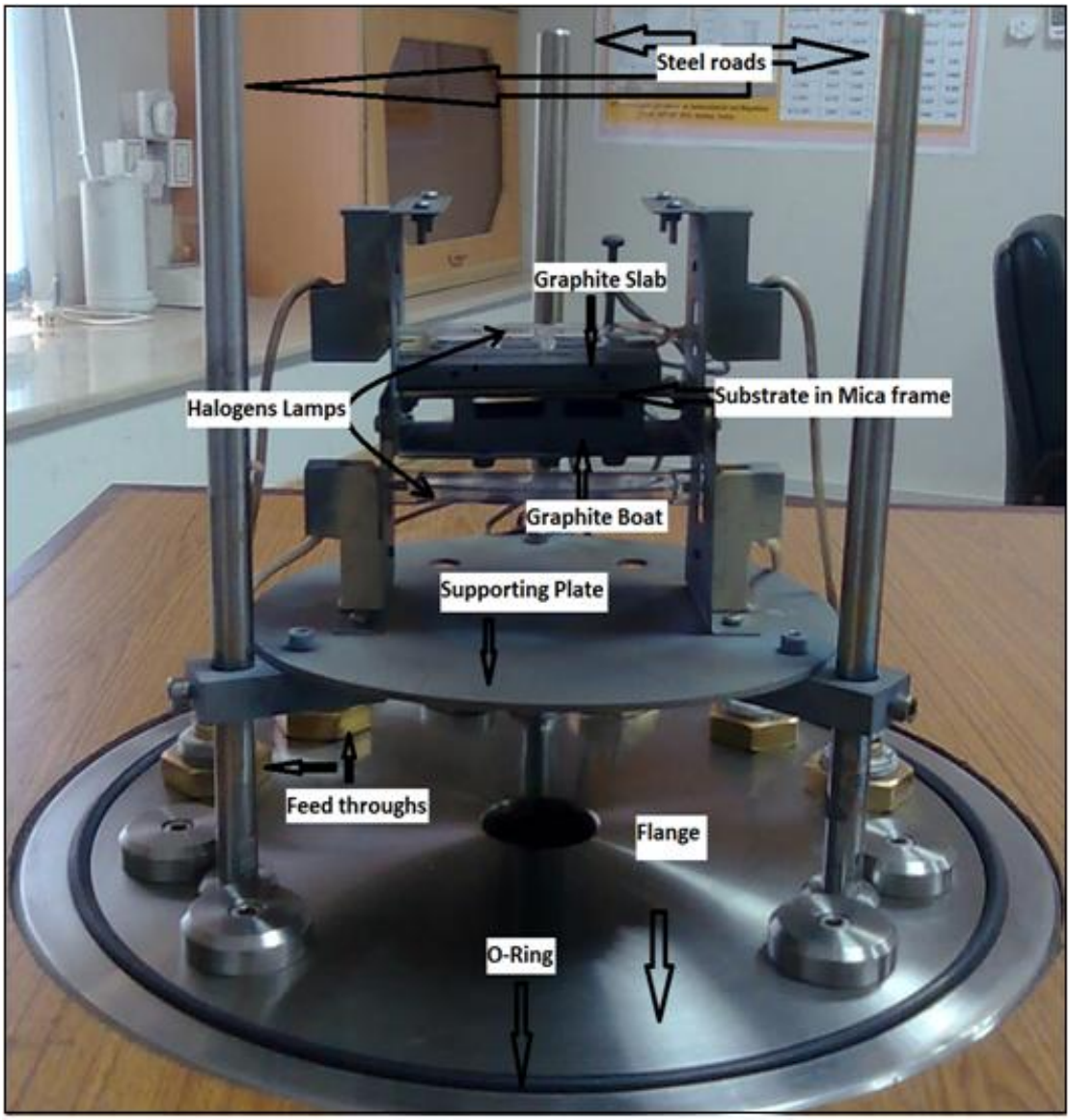

Figure 5.2: Internal view of CSS equipment in during this project

A rotary vane vacuum pump (WS Automa) was attached to the chamber. Schematic of Rotary pump is shown in the figure 5.3. Rotary pump contains an eccentrically mounted rotor with spring-loaded vanes as shown in the adjoining diagram. During rotation the vanes slide in and out within the cylindrical interior of the pump, enabling a quantity of gas to be confined, compressed, and discharged through an exhaust valve into the atmosphere [10]. Upon rotation of the rotor, the spring-loaded blades follow the wall of the chamber, thus generating the pumping action. Oil is employed as a sealant as well as a lubricant between components moving within tight clearances of rotary pumps.

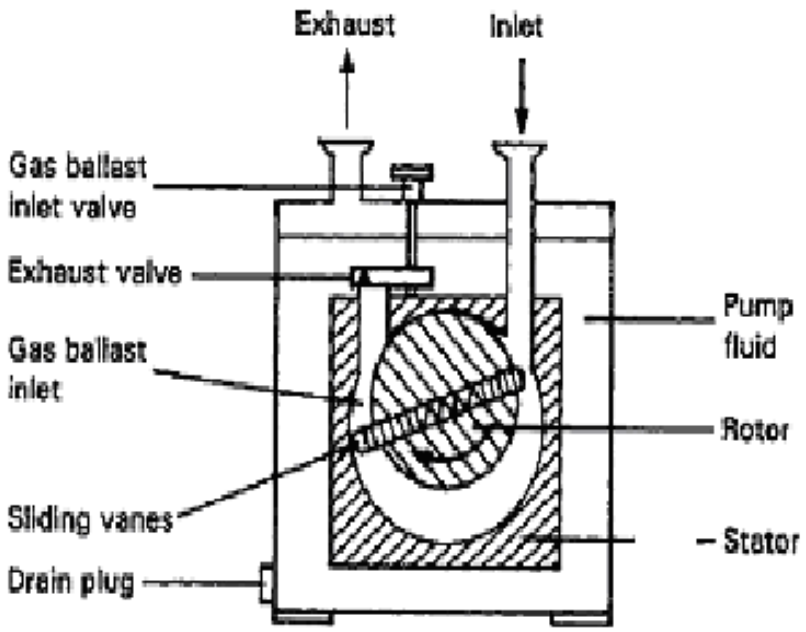

Figure 5.3: Schematic and working principle of Rotary Vane pump

Two valves were connected with the vacuum chamber, first was positioned between the pump and vacuum chamber to control the pumping rate and second to vent (when chamber requires to be opened) or give an inlet to an inert gas (when an ambient of a specific gas is required.

The pressure in the chamber is measured by a Pirani gauge unit (Gauge Head and Display Unit), which has a measuring range 10^{+3} – 10^{-3} mbar. The working principle of Pirani gauge is based on the thermal conductivity of gases. Internal schematic is shown in the figure 5-4. A heated metal filament suspended, loses heat to the gas as its molecules collide with the filament. If the gas pressure is reduced, number of molecules present decreased and the temperature of filament is increased due to the reduced cooling effect. Fewer collisions mean less heat is removed from the filament and it heats up. As it heats up, its electrical resistance increases.

The electrical resistance of a wire varies with its temperature according to the following formula;

$$\mathbf{R\,(T) = Ro\,(1+\alpha T)}$$

Where R(T) is resistance at T ^{0}C, R_0 is resistance at 0 ^{0}C and α is temperature co-efficient of filament metal e.g. 0.0046 $^0C^{-1}$ for tungsten.

Thus, if the resistance of the tungsten filament is measured, this can be related to its temperature and therefore, the pressure. A sensitive and convenient method of measure resistance is to use a Wheatstone bridge. The sensing filament in the gauge head forms one branch of a Wheatstone bridge and as the filament resistance changes upon collision of molecules, the bridge becomes out of balance. The out of balance detector sends a signal to the power supply causing the voltage to increase, making the filament to restore the temperature (110 ^{0}C). When it reaches at required temperature (110 ^{0}C), the bridge is again balanced and the detector signal decreases to zero. The voltage supplied by the power supply to keep the temperature constant, is calibrated on pressure scale. Such type of Pirani gauge is called temperature constant or resistance constant Pirani gauge [11].

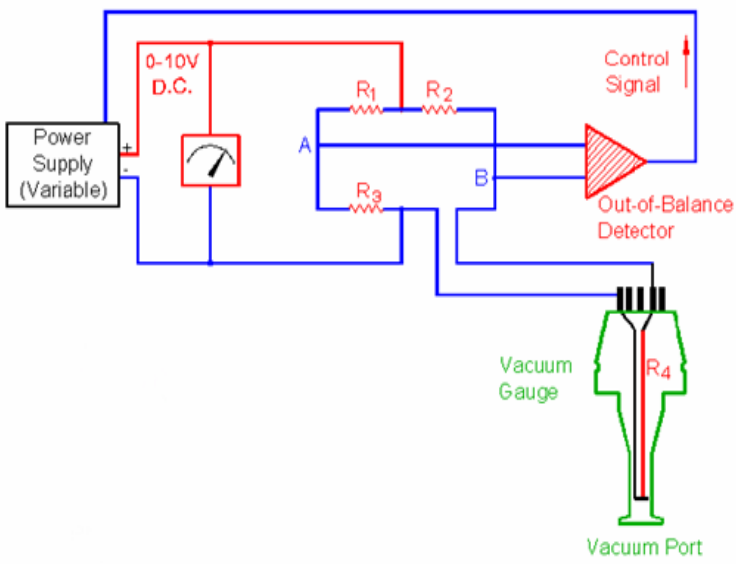

Figure 5.4: Schematic of Pirani gauge

5.3. DEPOSITION OF THIN FILMS BY CSS TECHNIQUE

Powder of a material (to be deposited) is poured and dispersed uniformly in the graphite boat. Mica sheet is used as a substrate holder and thermal insulator between source and substrate. The distance between source and substrate could easily be changed permitting optimal distance, in order to get required deposition rate and better uniform films. The substrate temperature is raised till the sublimation temperature under vacuum (10^{-2}-10^{-3} mbar), which is being attained in this chamber with the help of a rotary pump. The source temperature is adjusted lower than the substrate temperature so the vapors may travel from source to substrate. Temperature controllers have been attached with help of k-type thermo couples to monitor the temperatures of source and substrate. Thin films of different thickness are obtained by CSS, as thickness monitor can't be installed with this apparatus, due to narrow space between source and substrate

5.3.1. ADVANTAGES

1. The evaporation source and substrate are heated directly by halogen lambs and their temperature is controlled with temperature controllers.
2. The source and substrate are separated by a mica sheet of about 1-3mm. In this way the source vapors are confined to closed space, leads to less wastage of evaporated material as compared to other methods. The mica sheet keeps the source and substrate at different temperatures, due to which the evaporating material will always have better access to the substrate.
3. The distance between the evaporation source and substrate can easily be varied, permitting in this form to find the optimal separation (5-20mm).
4. The films deposited by this method present a high crystallographic orientation and adequate opto-electrical properties for photo voltaic applications.
5. The system is very simple and easy to handle.
6. It has high transport efficiency conducted under low vacuum conditions at moderate temperature.

5.3.2. LIMITATIONS

1. The main disadvantage of CSS deposition system is that there is no crystal monitor to check the growth rate and thickness of the film deposited.
2. This method can only be used for limited number of materials i.e. materials which can be sublimated at low temperatures [1].

REFERENCES:

[1] Z. Ali, “Fabrication of II-VI Semiconductor Thin Films and a Study of Structural, Optical and Electrical Properties”, Ph.D. Thesis, Quaid-i-Azam University, 2005

[2] B. R. Wakeling, “Close space sublimation of CdTe for solar cells and the effect of underlying layers”, Ph.D. Thesis, Cranfield University, 2009

[3] V. Kumar, “Characterization Of Large Area Cadmium Telluride Films And Solar Cells Deposited On Moving Substrates By Close Spaced Sublimation”, Ph.D. Thesis, University of South Florida, 2003

[4] T.Anthony, A.Fahrenbruch and R. Bube, “Growth Of CdTe Films By Close Spaced Vapor Transport”, J. Vac. Sci. Technol. A 2 (3), pp 1296-1302,1984

[5] H. Nagayoshi and K. Suzuki,” in IEEE Nuclear Science Symposium Conference Record” (2004), vol. 1-7, p. 4411.

[6] C.S. Ferekides, D. Marinskiy, V. Viswanathan, B. Tetali, V. Palekis, P. Selvaraj and D.L. Morel, “High ef®ciency CSS CdTe solar cells”, Thin Solid Films 361-362 (2000) 520-526

[7] S. Larramendi a, F.C.Zawislak b, M.Behar b, E.Pedrero a, M.Herna´ndez Ve´ lez c,d, O.deMelo, “Growth of ZnTe and CdTe films using the isothermal close space sublimation technique in vacuum environment”, Journal of Crystal Growth 312 (2010) 892–896

[8] http://www.suppliersonline.com/propertypages/304.asp

[9] http://www.azom.com/Details.asp?ArticleID=965

[10] M. Ohring, The Materials Science of Thin Films, Academic Press, California (1992)

[11] S.W. Husain, Vacuum Science and Technology, Code No. 1718.

CHAPTER 6

FABRICATION AND EFFECT OF INDIUM DOPING ON PROPERTIES OF CDS THIN FILMS

INTRODUCTION

In this chapter, we will study CdS thin films fabricated by Close Space Sublimation (CSS), effect of Indium (In) doping on the structural, morphological, optical and electrical properties of these thin films. CdS thin film is a very desirable window layer for many photovoltaic solar cells because of its optical and electrical properties [2–5]. CdS thin films are the most commonly used window material for high-efficiency CdTe and CuInSe2 polycrystalline thin film photovoltaic devices [11]. Efficiencies close to 16% have already been reported for CdTe/CdS thin film solar cells [12, 13].

Un-doped CdS thin films generally have high electrical resistivity. An effective way to produce less resistive n-type CdS films is by In doping [1]. It was seen that the resistivity in In-doped CdS films decreased and high-conductivity was obtained.

6.1.FABRICATION OF CdS THIN FILMS BY CSS TECHNIQUE

Transparent orange yellow colored thin films were obtained by close space sublimation unit (installed at TFTR Laboratory @ COMSATS, Islamabad). Soda lime glass was used as a substrate to deposited CdS thin films on it. Before the fabrication of thin film, glass substrate was ultrasonically cleaned in IPA bath. CdS powder (99.99% pure) was used to sublimate from a graphite boat (as explained in Chapter 4). Mica sheet was used as a substrate holder and thermal insulator between source and substrate. The distance between source and substrate could easily be changed permitting optimal distance, in order to get required deposition rate and better uniform films. During this experimentation, the source and substrate were separated by a distance of 15mm. The source and substrate were kept at 550 ^{0}C and 400 ^{0}C respectively. The pressure of the evaporation chamber was $\approx 10^{-4}$ mbar.

Transparent yellowish thin films of different thickness were obtained, as there is no thickness monitor installed in this apparatus to control the thickness. Films had good adhesion with the glass substrate, as tested by squash tape test. These films were thermally annealed at 400 ^{0}C in a vacuum chamber having a pressure of $\approx 10^{-2}$mbar. Each sample was cut into two pieces,

one to characterize (Compositional, Morphological, structural, optical and electrical) before doping and second for after doping, as explained in coming sections.

6.2.INDIUM-DOPED CdS THIN FILMS

CdS thin films fabricated by CSS method were doped with indium to decrease their resistivity without changing type of careers (i.e. n-type). Resistive evaporation method was used to deposit 40nm thin layer of Indium on each CdS film by Edward 610A coating unit present at Optics Laboratory, PAEC, Islamabad.

The deposition rate was 1 nm/s on the following parameters; pressure inside the chamber: $\leq 10^{-5}$ mbar, source and substrate temperatures were 270 ^{0}C and 28 ^{0}C respectively. Thickness of the films was monitored by quartz crystal thickness meter.

6.3.ANNEALING OF IN/CdS/GLASS THIN FILMS

Mainly, Annealing was performed in order to diffuse the In atoms in CdS films. CdS thin films coated with an evaporated In layer, were thermally annealed in vacuum and we observed that In layer was disappeared by evaporation rather to diffuse in the CdS films. To stop the evaporation of In into air and force to diffuse in the CdS thin films, we thermally annealed the samples in air rather in vacuum. These samples were thermally annealed at several temperatures; 200 ^{0}C, 250 ^{0}C, 300 ^{0}C, 350 ^{0}C, 400 ^{0}C, 450 ^{0}C, 500 ^{0}C in a Muffle furnace. The effects of the thermal annealing process on structural, electrical, optical properties and In content to be diffused in the CdS layer with varying temperature were studied. We found that the thermal annealing in air produces an external layer of In_2O_3 which stops the evaporation of In into air, further formation of In_2O_3 hence, remaining In atoms start to diffuse in CdS layer. S.J. Castillo et al showed that for an annealing temperature of 250 ^{0}C, most of the top In layer is oxidized, leaving a lower amount of it in a transition zone with the CdS film [6]. The results showed that the samples annealed at higher temperatures (300 ^{0}C, 350 ^{0}C, 400 ^{0}C), structure of the form In_2O_3-voids/In_2O_3-CdS/CdS-In/glass is observed.

6.4.CHEMICAL ETCHING

Some annealed samples in air, were immersed in diluted HNO3 solution for a few seconds in order to etch the oxide external layer. In this way it was possible to measure the electrical resistivity of the In:CdS layer in the annealed samples.

6.5.RESULTS AND DISCUSSIONS

In the following section, results obtained from different characterization techniques (morphological and elemental composition, structural, optical and electrical) will be discussed that how the results obtained are related to the previously reported literature.

6.5.1. ELEMENTAL COMPOSITION

The composition of the CdS films deposited on glass substrate was determined by EDX measurements, using the ZAF algorithm based calculations. Attention was placed on checking the atomic ratio between constituting elements to get information about stoichiometry of films. Actual atomic ratio between the elements Cd and S in CdS should be 1:1. But CdS films deposited by CSS are not stoichiometric. Sulfur is slightly less (5.48 atomic %) than its actual atomic percentage as shown in the figure 6.1, accompanied by a table 6.1. This might be due to the decomposition during evaporation of CdS from source to the substrate. As a result, the CdS films obtained by CSS are Cd-enriched (Cd is 5.48 % more than sulfur), which is ultimately useful for the lowering of resistivity of the CdS films. As the highly stoichiometric films have higher resistivity as compared to Cd-enriched.

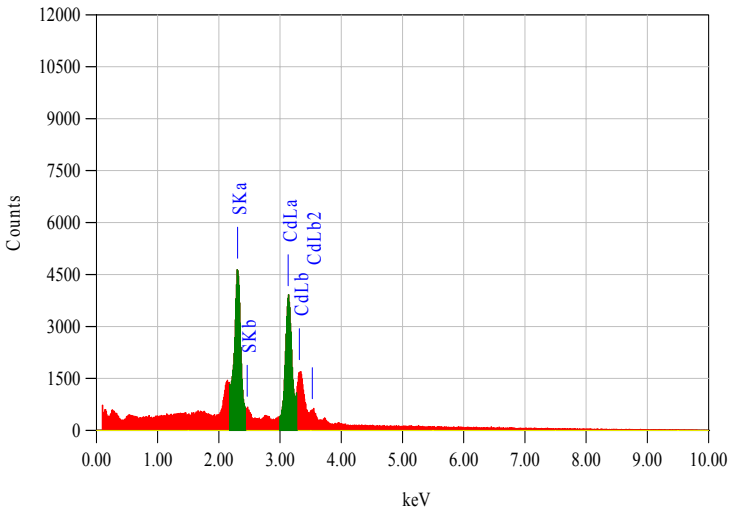

Figure 6.1: EDX spectrum collected for as-deposited CdS film by C

Table 6.1:

ELemental composition of as-deposited CdS obtained from EDX

Element	Error %	Atomic %
Cd	0.42	55.42
S	0.08	44.58
Total		100.00

Figure 6.2 shows the EDX spectrum of In evaporated CdS film annealed 450 ^{0}Cin air. Spectrum is showing that 18.21 at. % of In is present. Composition of rest of the samples is given in the table 5.1 which confirms the presence of In in each sample.

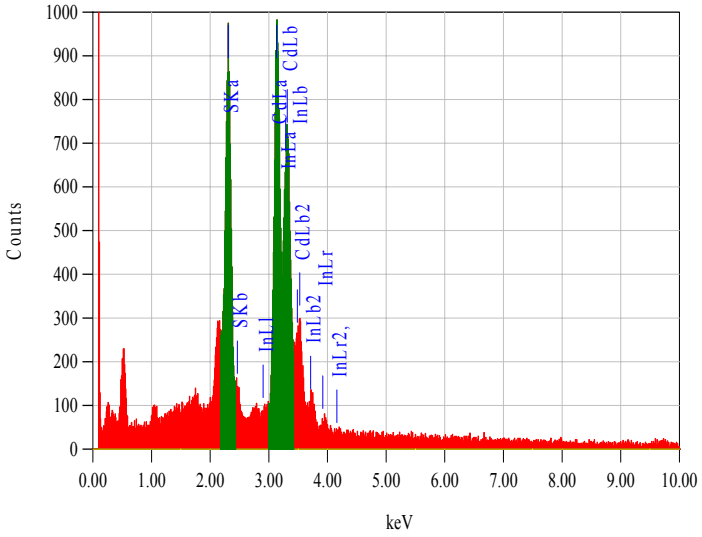

Figure 6.2: EDX spectrum collected for In-doped CdS film

Table 6.2:
Elemental composition of In-doped CdS samples obtained from EDX

Sample	Annealing Temperature (^{0}C)	Elemental Composition			
A	300	Element	Cd	S	In
		Atomic %	45.66	36.17	18.08
B	350	Element	Cd	S	In
		Atomic %	46.67	34.53	18.80
C	400	Element	Cd	S	In
		Atomic %	17.64	7.46	74.90
D	450	Element	Cd	S	In
		Atomic %	45.97	35.82	18.21

6.5.2. SURFACE MORPHOLOGY

Surface morphology of the samples was observed by Scanning Electron Microscope. As-deposited CdS thin films are highly resistive (up to 10^8 Ωcm) that's why image of samples was drifting due to accumulation of electrons on the surface of sample acting like a mirror. To avoid this situation, we evaporated 200 Å layer of gold on CdS thin films to make their surface conductor and grounded it with help of aluminum tape. SEM micro-graph of as deposited sample in the figure 6.3 shows uniform sized clusters which are made up of closely packed nano particles (crystallite size of ≈ 48 nm; determined by XRD) is observed.

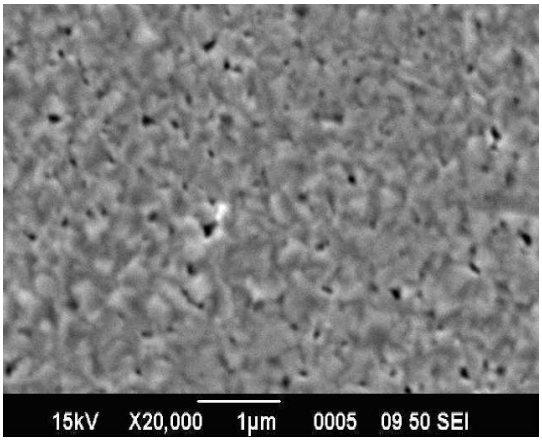

Figure 6.3: As-deposited CdS film on a glass substrate.

Figures 6.4 to 6.7 are showing In evaporated samples annealed in air for one hour at various temperatures. A gradual change is observed in the surface morphology; as the annealing temperature is increasing, morphology is becoming rough. This is due to the fact that at lower temperature pure In is present on the surface giving a smooth and uniformly sized grains morphology. As the annealing temperature is increased indium starts to diffuse inside the CdS and remaining is converted to In_2O_3 which has also been proposed by S.J. Castillo et al. [6]. Further annealing gave more complex oxides of CdS, observed in XRD results.

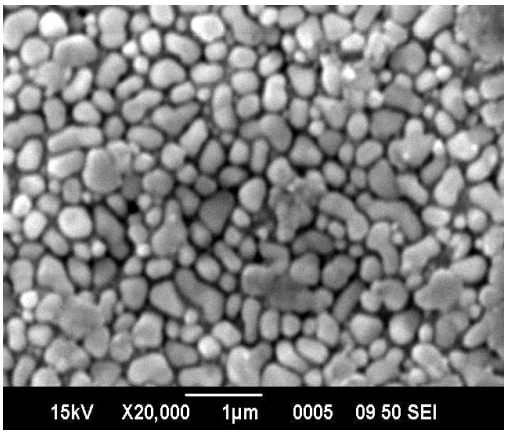

Figure 6.4: In:CdS; annealed at 300 ^{0}C

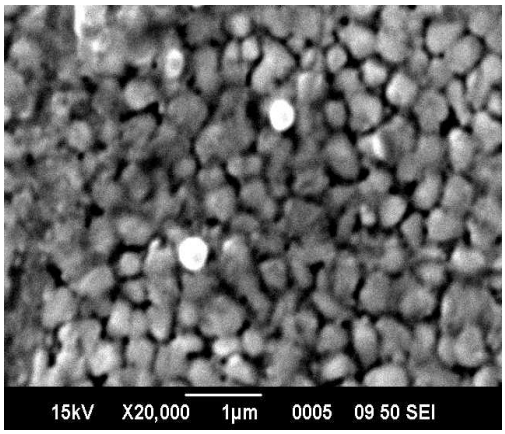

Figure 6.5: In:CdS; annealed at 350 ^{0}C

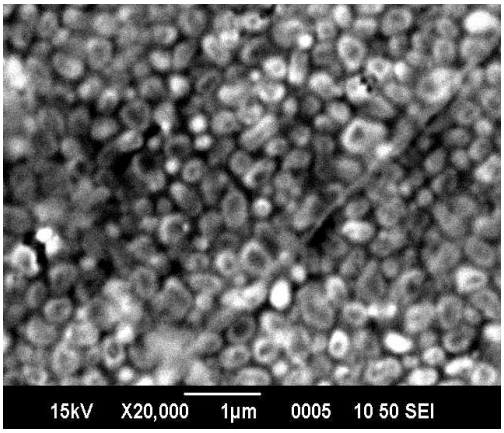

Figure 6.6: In:CdS; annealed at 400 ^{0}C

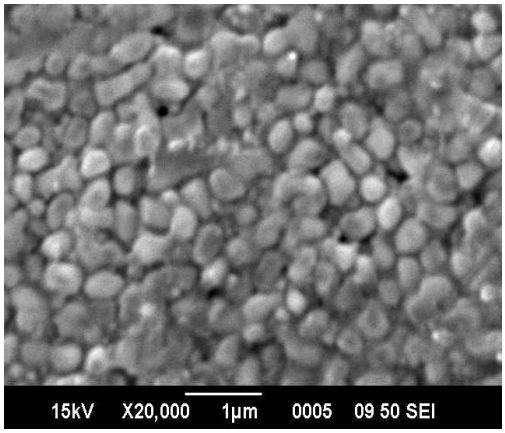

Figure 6.7: In:CdS; annealed at 450 ^{0}C

6.5.3. STRUCTURAL PROPERTIES

Figure 6.8, shows the XRD patterns of as-deposited sample; we found two types of crystal structures of as-deposited CdS which are Cubic and Hexagonal, as reported in the literature review. CdS thin films obtained by CSS have Cubic (1 1 1) preferential site of growth found at 26.5^0(2 Theta). Two small peaks of CdS having hexagonal structure are found at 47.80 and 75.4,

as shown in the figure 6.8. This confirms that pure CdS thin films have been obtained by CSS method.

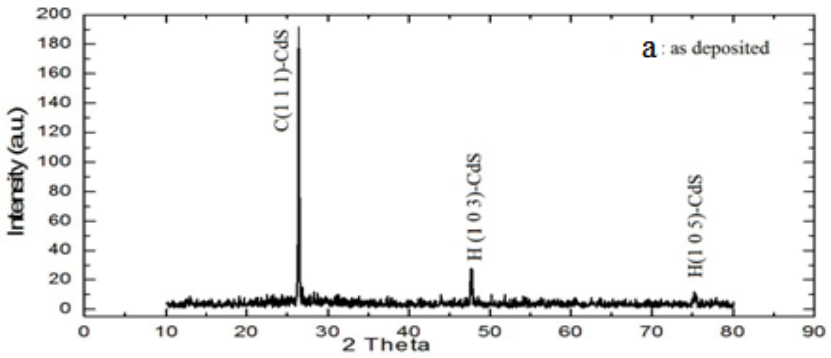

Figure 6.8: XRD results of as deposited sample Samples

Figure 6.9 is showing results of samples annealed in air for one hour at different temperatures. The strongest diffraction peaks are C(1 1 1), approximately at 27^0 and the T(1 0 1) approximately at 33^0 for CdS and In respectively. One of the effects of the thermal annealing is the oxidation of In, this can be seen in the X-ray patterns of the samples annealed between 300 ^{0}C and 400 ^{0}C. In these patterns, diffraction lines of In appear at approximately 33^0 corresponding to T(1 0 1) and T(2 0 2). Mean-while, the diffraction lines of In disappear, annealing at 350 ^{0}C. This can be explained in terms of the oxidation of the In layer surface exposed to the air during the annealing. Diffraction peak corresponding to R(1 1 0) of In_2O_3 is appeared at 32.6^0 at annealing temperature of 400 ^{0}C. This oxide layer grows from the In layer with increasing the annealing temperature. The amount of In decreases with annealing temperature due to the partial conversion into the oxide and also due to the partial diffusion into the CdS layer which is manifested by the presence of diffraction lines of $CdIn_2S_4$. The external oxide layer prevents from the outward In diffusion or evaporation and from the oxidation of the CdS layer. However, the oxidation of Cd begins at 350 ^{0}C as manifested by the presence of a weak diffraction peak of CdO corresponding to C(1 1 1) at 33^0. At annealing temperatures higher than 350 ^{0}C some complex oxides were found and no pure or compound of In was detected after annealing at 450 ^{o}C, as shown in the figure 6.9.

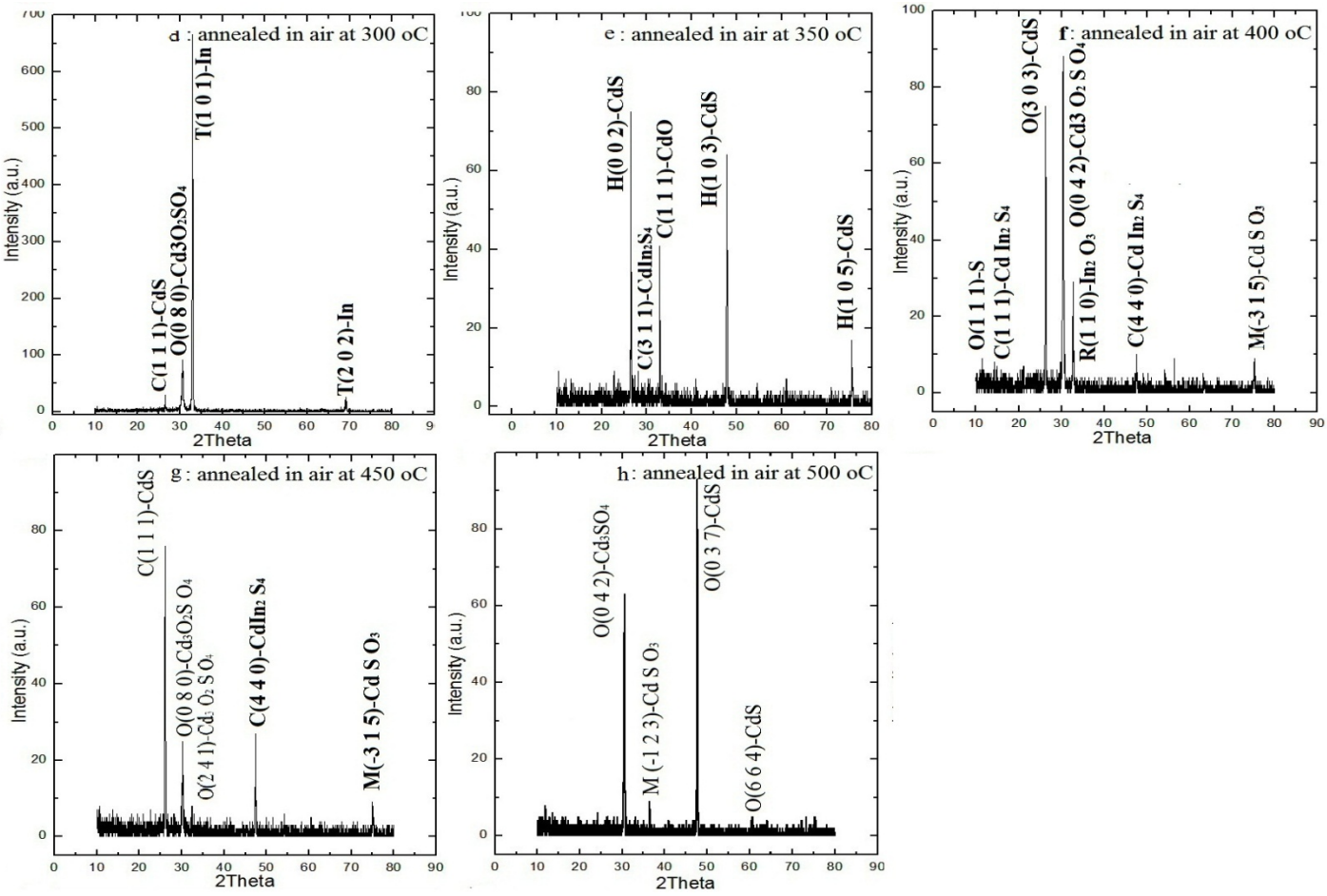

Figure 6.9: XRD patterns of In/CdS/glass samples annealed in air at 300^{0}C, 350^{0}C, 400 ^{0}C, 450^{0}C and 500^{0}C

Hence, It is to be concluded from the XRD patterns obtained that relatively better results are obtained between 300 0C to 400 ^{0}C for In diffusion in the CdS films.

6.5.4. OPTICAL PROPERTIES

Transmission or transmittance is the only property which is obtained directly from the film and the rest are inferred from the transmission spectra.

The as-deposited films of various thicknesses are showing transparency from 50% to 85% in the region of visible, IR and NIR, as shown in the figure 6.10. There's no transmission in the ultraviolet region. While moving from ultraviolet to visible, a sudden rise in transmission about the wavelength of *500* nm is observed which reveals that, the band-gap of CdS occurs in this region. For rest of region (visible infrared and near infrared), CdS is working as a window

layer. The one more study, we are getting from figure 6.10 is; as the thickness of the films is increasing, transmission is decreasing. As the thickness is increased, there are more chances for scattering and absorption of light while transmitting through the material. This is one of the main reasons for decreasing in transmission with increasing thickness.

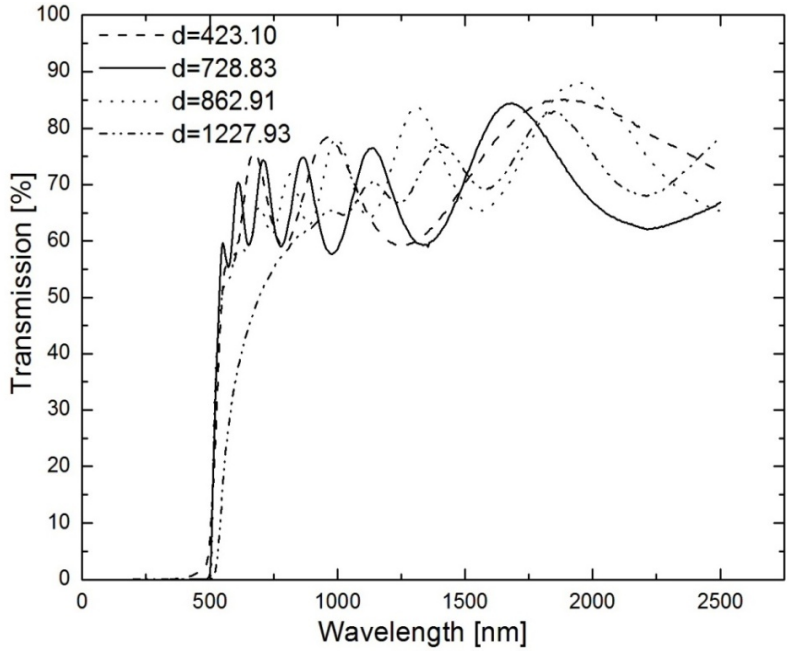

Figure 6.10: Optical transmission of as-deposited samples of various thicknesses

Figure 6.11 is showing the transmission of Indium evaporated CdS samples, annealed in air at various temperatures for the diffusion of Indium atoms into the CdS films. In doped CdS films are showing the transmission from 15% to 70% depending upon the annealing temperature. In case of as-deposited samples, transmission is 50% to 70%. As the samples has been evaporated with 40nm of In layer which reflects most of the light back. This is very clear from the figure 6.11 that with increasing the annealing temperatures, transmission is improving. As the annealing temperature is increased more and more In atoms diffuse inside the CdS films from surface, leaving less amount on the surface. Back reflection of light cannot be avoided completely from In atoms even when all the atoms diffuse in the films because diffused atoms also take a part in reflection but relatively smaller then the In atoms on the surface.

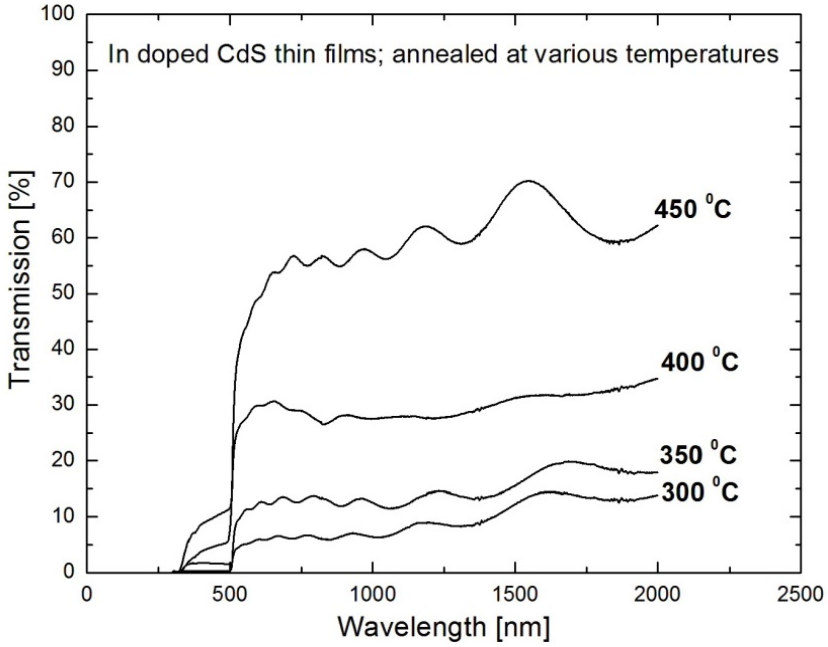

Figure 6.11: Optical transmission of In-doped samples, annealed in air at various temperatures

The band gap of the films was determined by using the well-known relation for direct band gap: $hv = A(hv - E_g)^{1/2}$, where A is a constant, hv is the photon energy and E_g is the band gap (energy gap) [7]. Band gap; E_g was obtained by extrapolating $(\alpha hv)^2$ vs. the incident photon energy (hv), as shown in the figure 6.12 for as deposited. The value of band gap for as-deposited samples is very close to the previously reported value i.e; 2.4eV [8]. Details of the other as-deposited samples are shown in the table 6.1.

After In doping band gap is not much affected. Its value varies from 2.35eV to 2.43eV which is almost constant. Figure 6.13 is showing the determination of band gap for In-doped CdS thin films. Details of other samples; annealing temperature and band gap are given in the table 6.2.

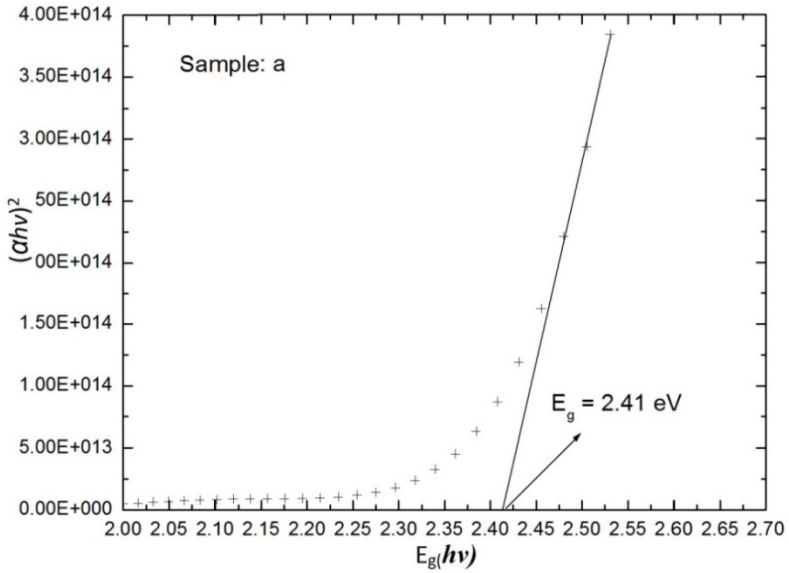

Figure 6.12: Determination of band gap of as-deposited samples by extrapolating $(\alpha hv)^2$ vs. (hv)

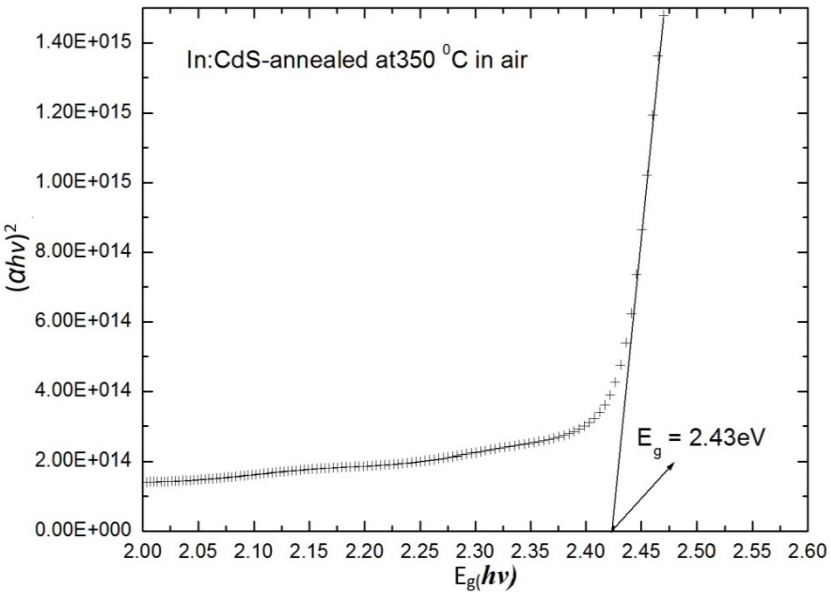

Figure 6.13: Determination of band gap of In-doped samples by extrapolating $(\alpha hv)^2$ vs. (hv)

Figure 6.14 is revealing the dependence of refractive on film thickness; as the film thickness is increasing refractive index is decreasing. This analysis was performed by using four selected samples of different thickness and curve fitting (b-spline) gave the trend; how refractive index is decreasing with the increase of film thickness.

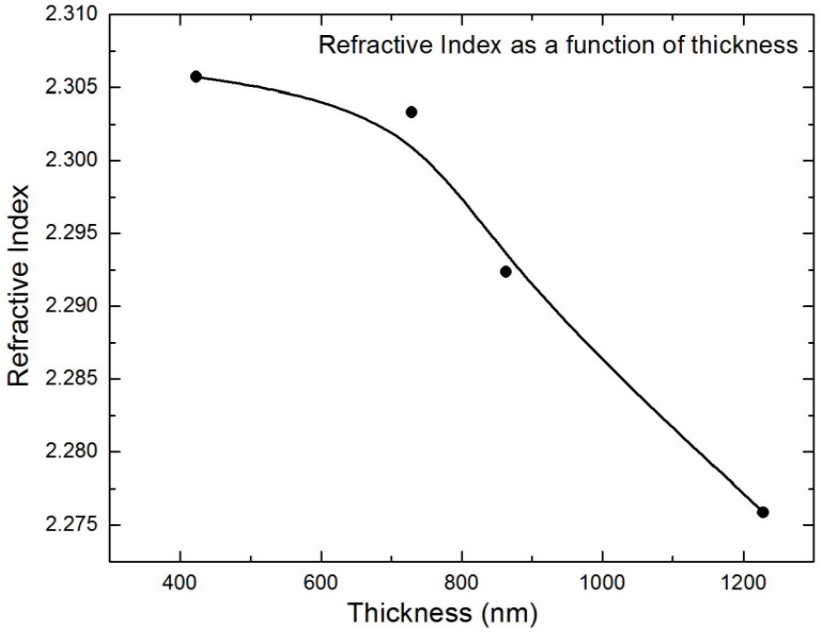

Figure 6.14: Refractive index as a function of film thickness; Refractive index is decreasing with increasing thickness of films

Table 6.3:

Thickness, Refractive Index and Band gap of as-deposited samples

Sample	Thickness (nm)	Refractive Index	Band gap (eV)
A	423.10	2.31	2.41
B	728.83	2.30	2.43
C	862.91	2.29	2.44
D	1227.93	2.27	2.31

Table 6.4:

Band gaps of In-doped samples annealed at various temperatures

Sample	Annealing Temperature (^{0}C)	Band gap (eV)
A	300	2.35
B	350	2.43
C	400	2.38
D	450	2.42

Hence, it is to be concluded from the optical spectra and calculations based upon them, relatively better results (high transmission) are obtained at higher temperatures.

6.5.5. ELECTRICAL PROPERTIES

As-deposited CdS thin by CSS method on a glass at substrate temperature of 400 ^{0}C were n-type and have a resistivity of 10^4-10^6 Ωm; which reveals that the films are highly stoichiometric and to reduce their resistivity, CdS films were doped with In. Hall Measurement system (Ecopia HMS 3000) was used to measure the electrical properties (electrical resistivity, mobility and Hall Coefficient) before and after doping. Silver paste was used to make ohmic contacts on the surface on films. CdS films of different thickness were obtained by CSS method. In the figure 6.15, the dependence of resistivity of as-deposited samples on the film thickness is shown. Resistivity was plotted vs. thickness of the films and curve fitting (b-Spline) gave the pattern of how the resistivity is decreasing with increasing thickness. With the increasing film thickness, grain size also increases which leads to the decrease of defects so that the resistivity is also decreased [9]. Table 5.3 is showing the resistivity and mobility of as-deposited samples of various thicknesses.

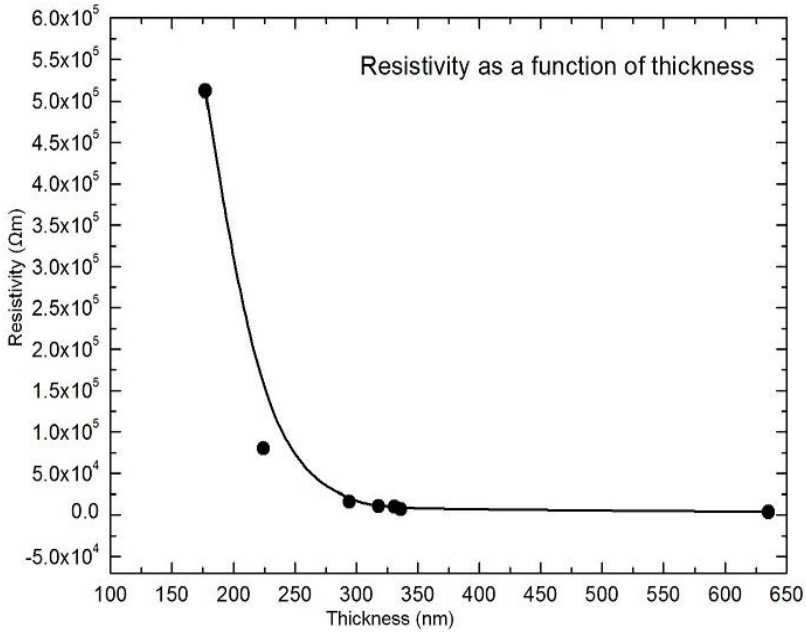

Figure 6.15: Resistivity as function of film thickness; Resistivity decreases as the film thickness increases

Table 6.5:

Resistivity and mobility of as-deposited samples of various thicknesses

Sample	Thickness (nm)	Resistivity (Ωcm)	Mobility (cm^2/Vs)
1	177	5.12×10^5	2.502×10^0
2	224	8.02×10^4	2.213×10^2
3	294	1.61×10^4	1.217×10^3
4	318	1.11×10^4	1.94×10^1
5	331	9.95×10^3	2.253×10^1
6	336	7.37×10^3	5.93×10^2
7	635	3.79×10^3	1.208×10^3

The temperature dependence of current and resistivity was measured by four probe method, using a KEITHLEY 2400 source meter. Samples were put into a vacuum chamber of pressure $\approx 10^{-3}$ mbar. A constant voltage was applied and varying the temperature, the change in current was noted. Increasing the temperature leads to increase in current as well. This confirms

the semiconductor behavior of CdS thin films, as shown in the figure 6.16. A linear regression line with a good fitting coefficient is showing increasing behavior of current with temperature. Resistivity of the sample was used by calculating the resistance from current and voltage applied and hence from resistivity. Increase in temperature leads to decrease in resistivity, as the charge carriers are activated by increasing the temperature in semiconductors, as shown in the figure 6.17. A polynomial of degree three is revealing the decreasing behavior of resistivity with increasing current

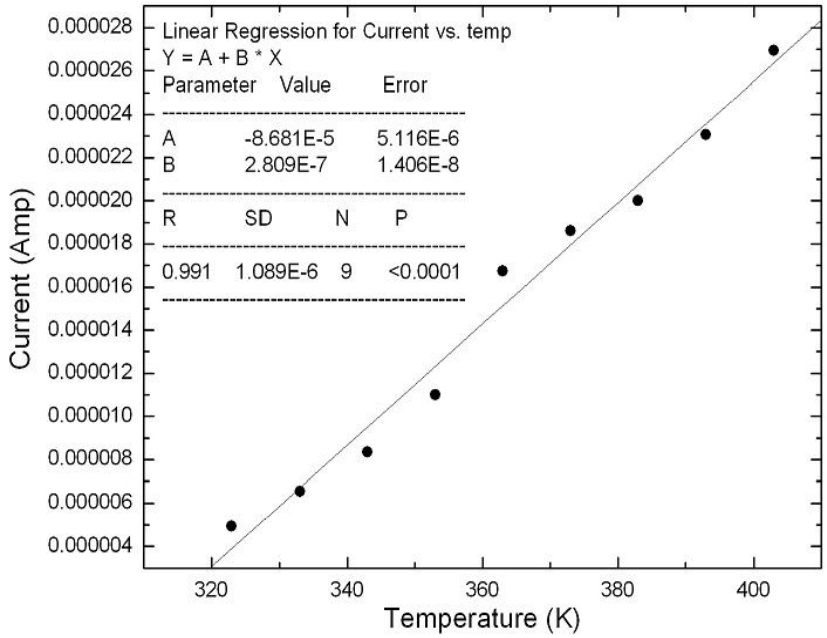

Figure 6.16: Temperature dependence of current

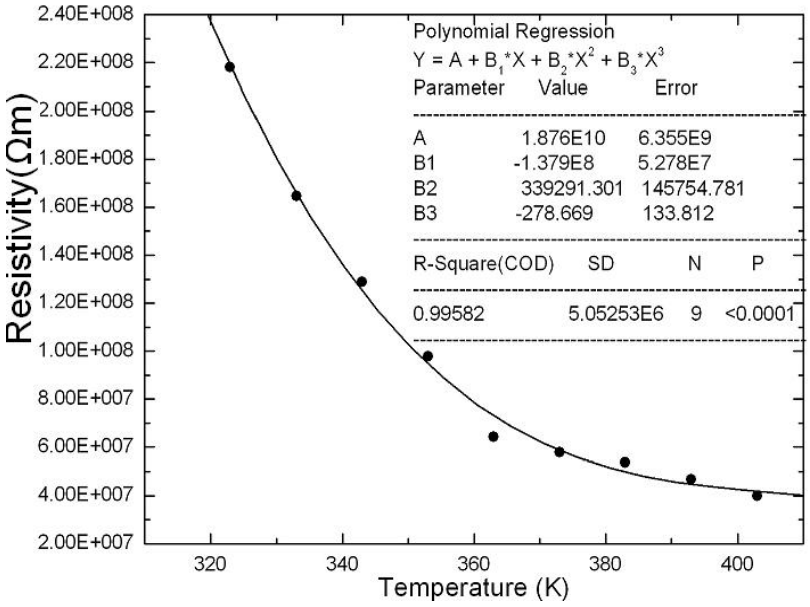

Figure 6.17: Temperature dependence of resistivity

The conductivity might be represented by the following relation [10],

$$\sigma = \sigma(0) \exp[-(\Delta E)/ k_B T]$$

Where ($\Delta E \equiv E_f - E_v$) represents the activation energy and $\sigma(0)$ is the conductivity at $1/T = 0$. The activation energy (ΔE) was calculated by plotting ln (σ) vs. $1/k_B T$, where the slope of linearly curve fitted regression gives the activation energy as shown in the figure 6.18. The conductivity activation energy of as deposited sample comes out to be 894.234J.

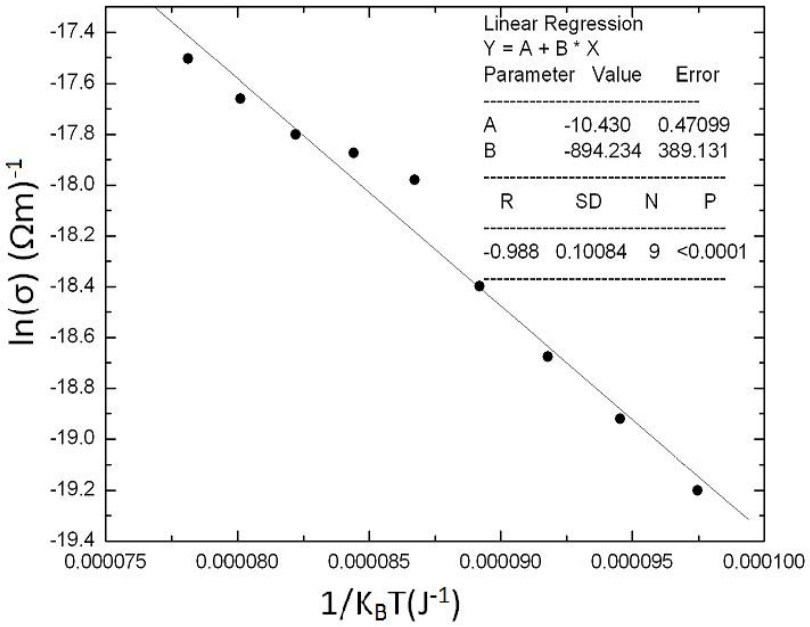

Figure 6.18: conductivity activation energy of as deposited sample

CdS films evaporated with 40 nm of In layer were thermally annealed in air for one hour at various temperatures for the diffusion of In into CdS films. It was ensured from XRD results that greater the annealing temperature (up to 400 ^{0}C) greater will be the diffusion of In atoms in the CdS films. These heat treated samples were chemically etched in the diluted HNO_3 solution to remove the In_2O_3 layer formed on the surface so we may find the resistivity of In:CdS films. DC electrical resistivity of the samples was measured before and after etching. A decrease in resistivity confirms the removal of oxide layer from the top surface. The resistivity of In:CdS samples were measured to be 10^{-1}-10^{-2} Ωm without changing the type of current carrier (i.e; n-type). This decrease in resistivity might be due to the formation of new compounds; such as $CdIn_2S_4$ and In atoms in the films which were confirmed from XRD results.

Figure 6.19 shows the variation in resistivity by increasing the annealing temperature of films. Initially, resistivity decreased by increasing the annealing temperature which shows that increasing the annealing temperature results in increased quantity of In diffusion in the films. After a lowest value of resistivity ($\approx 10^{-2}$ Ωcm) at temperature 400 ^{0}C, it again starts to increase. This might be due to the formation of complex oxides of CdS confirmed by XRD results. Figure 6.20 shows the variation of mobility with increasing annealing temperature. Mobility is showing the inverse behaviour to resistivity by increasing the annealing temperature. Reason is that the

decrease in resistivity results in increase of mobility. Resistivity and mobility values corresponding to annealing temperatures are shown in the Table 6.4

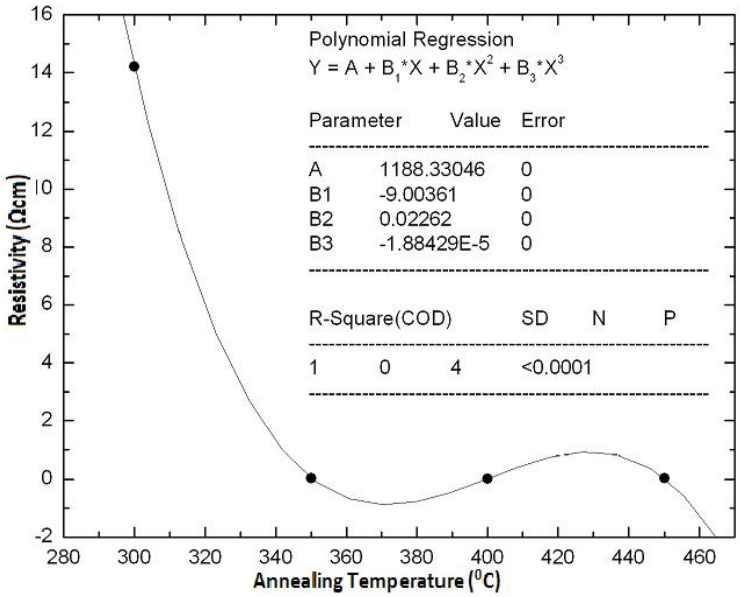

Figure 6.19: Variation in resistivity with annealing temperature of In-doped samples

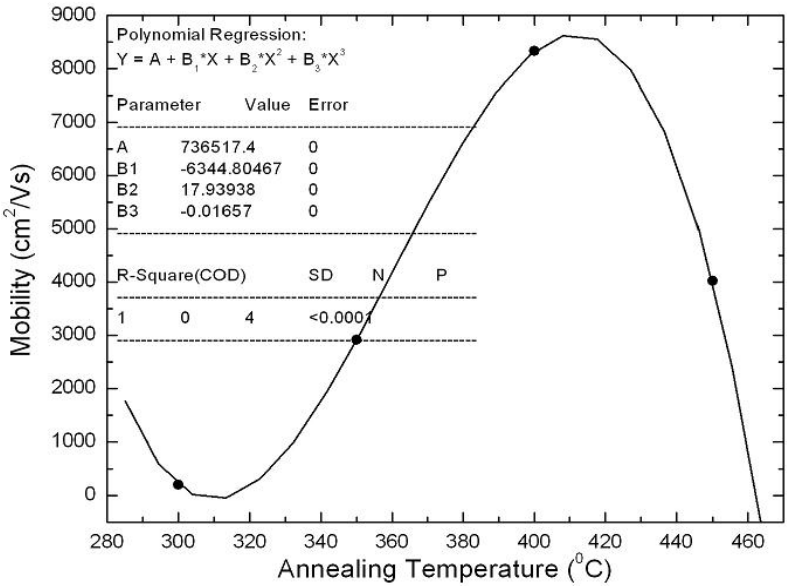

Figure 6.20: Variation in mobility with annealing temperature of In doped samples

Table 6.6:

Resistivity and Mobility of In-doped samples at different annealing temperatures

Sample	Annealing Temperature (^{0}C)	Resistivity (Ωcm)	Mobility (cm^2/Vs)
1	300 ^{0}C	1.422×10^{1}	1.942×10^{2}
2	350 ^{0}C	3.335×10^{-2}	2.913×10^{3}
3	400 ^{0}C	1.758×10^{-2}	8.331×10^{3}
4	450 ^{0}C	4.051×10^{-2}	4.017×10^{3}

The restults obtained from electrical characterization shows that the good results are obtained at an annealing temperature of below 450 ^{0}C. As at 450 ^{0}C, complex oxides of CdS films start to form which spoil the electrical as well as morphological properties.

REFERENCES

[1] F. Atay, V. Bilgin, I. Akyuz, S. Kose, Materials Science in Semiconductor Processing 6 (2003) 197–203

[2] Valyomana AG, Vijayakumar KP, Purushothaman C.Conductivity studies on spray-pyrolysed CdS films in ambient conditions. J Mater Sci Lett 1992;11:616–8.

[3] Chavez H, Jordan M, McClure JC, Lush G, Singh VP.Physical and electrical characterization of CdS films deposited by vacuum evaporation, solution growth and spray pyrolysis. J Mater Sci: Electr Mater 1997;8:151–4.

[4] Izci F, Kose S, K"yl"yckaya MS. Electrical, optical and structural properties of Cd1_xInxS films grown by spray pyrolysis method. Proc Suppl Bpl 1997;5:1115–9.

[5] Valyomana AG, Vijayakumar KP, Purushothaman C. Effect of annealing temperatures on the electrical transport properties of spray-pyrolysed CdS films. J Mater Sci Lett 1990;9:1025–7.

[6] S.J. Castillo, A. M. Galv´an, R. R. Bon, F.J. E, Beltran, M. S. Lerma, J. G. Hern´andez, G. Mart´ınezd, Thin Solid Films 373 _2000. 10]14

[7] N. A. Shah, A. Ali, Z. Ali, A. Maqsood, A.K.S. Aqili, J. Crys. Grow, vol.284, pp.477, 2005.

[8] H.M. Moller, Semiconductors for Sol. Cells, Artech House, Boston, 1993.

[9] E. Bertmana, J. L. Morenzaa and J. Estevea, Thin Solid Films **123** (1985) 297.

[10] J. B. Webb, D. E. Brodic, Can, J. Phys. 52(1974)2240.

CONCLUSIONS

In the present work, "Development of Closed space Sublimation Technique and Preparation of Cd-Based Thin Film", CSS Unit for the fabrication of CdS thin films was built and installed at Thermal Transport Laboratory, SCME, NUST, Islamabad. Good quality CdS films were fabricated on ultrasonically cleaned glass substrate by CSS. Adhesion of films on glass was attested by squash tape test.

SEM micro-graphs showed that films have smooth morphology with particle size ranging from 200nm to 400nm. EDX spectra revealed that CdS films are Cd-enriched (≈Cd: 55 at % and S: 45 at %). XRD results showed the polycrystalline growth (cubic and hexagonal) but preferred orientation of growth is Cubic (111). The resistivity of as-deposited CdS films was 10^3-10^5 Ωcm which is less than reported (>10^6 Ωcm) by the most of the researchers. This is due the Cd-enriched CdS film. Indium was doped to further decrease their resistivity (10^{-1}–10^{-2} Ωcm) without changing the type of carriers (n-type). As-deposited samples showed a transmission of 70% to 80% with an optical band gap of 2.42 eV. Slight decrease in transmission was observed after doping but most of the samples showed no change in band gap. Transmission seemed to be improved by increasing the annealing temperature. In doped CdS films gave the better results regarding optical and electrical properties at annealing temperature from 300 ^{0}C to 400 ^{0}C. In doped CdS films are suitable for window layer application in CdS/CdTe solar cells due to their low resistivity and high unaffected band gap.

FUTURE WORK

The CSS system could be modified to enable it to be used to get films of materials have high sublimation temperatures. Heating assembly of the system which is halogens lambs in the present situation can be replaced by resistive heating unit to get more temperature range. An electro-mechanical shutter can be installed between source and substrate to stop at once at a particular time. Further, CdS films could be obtained from different techniques like sputtering and then compare the properties of CdS films obtained by CSS and sputtering.